# ISOLDE: βDF

Многоканальное запаздывающее деление в области нейтронно-дефицитных изотопов свинца (ядра франция и астата)

ISOLDE, CERN

**А. Е. Барзах, П. Л. Молканов,**
**М. Д. Селиверстов, Д. В. Федоров**

# ISOLDE

**IS 466:**

Identification and systematical studies of the electron-capture delayed fission (ECDF) in the lead region - Part I: ECDF of $^{178,180}$Tl and $^{200,202}$Fr isotopes

**IS 534:**

Beta-delayed fission, laser spectroscopy and shape-coexistence studies with radioactive $_{85}$At beams

# ISOLDE: Laser Ion Source

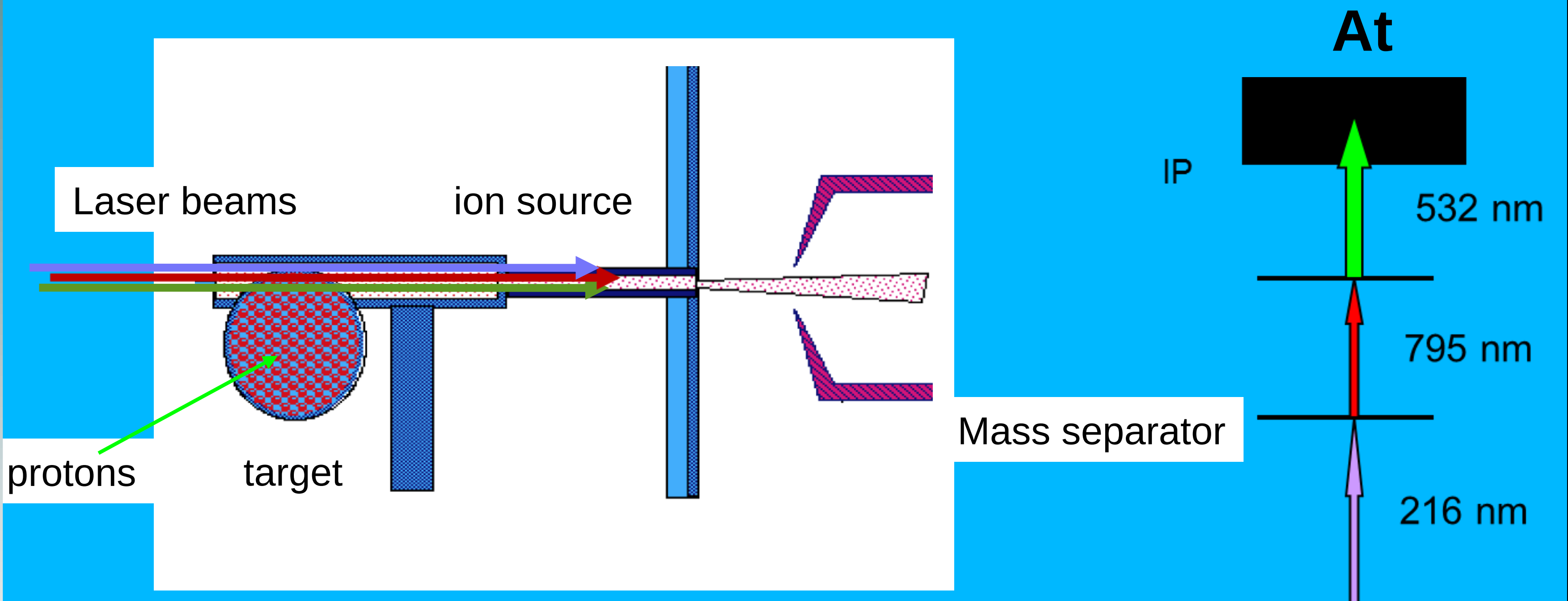


Laser Ion Source (LIS)

# Beta-delayed fission

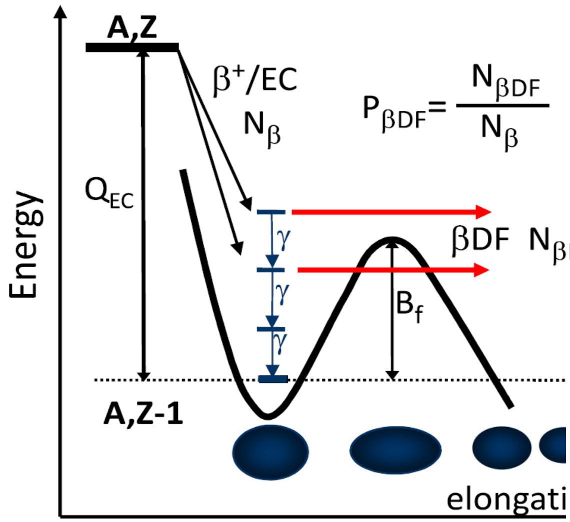


$Q_{EC}(A, Z) \gtrsim B_f(A, Z\text{-}1$

Nearly zero β-branch for lighter nuclei

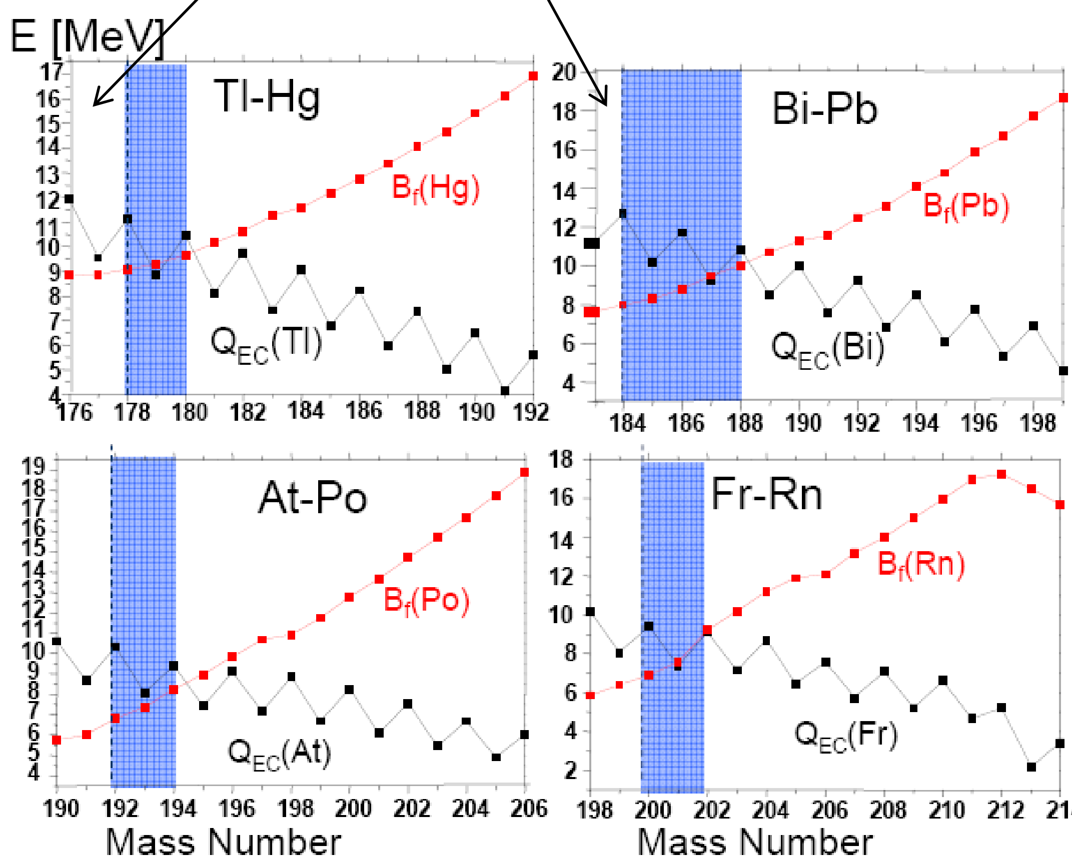


Observables:

$P_{\beta Df}$ ⟹ $B_f$,

fragment A/Z distribution,

mean TKE ⟹ elongation of the scission configuration

TKE distribution

# Beta-delayed fission

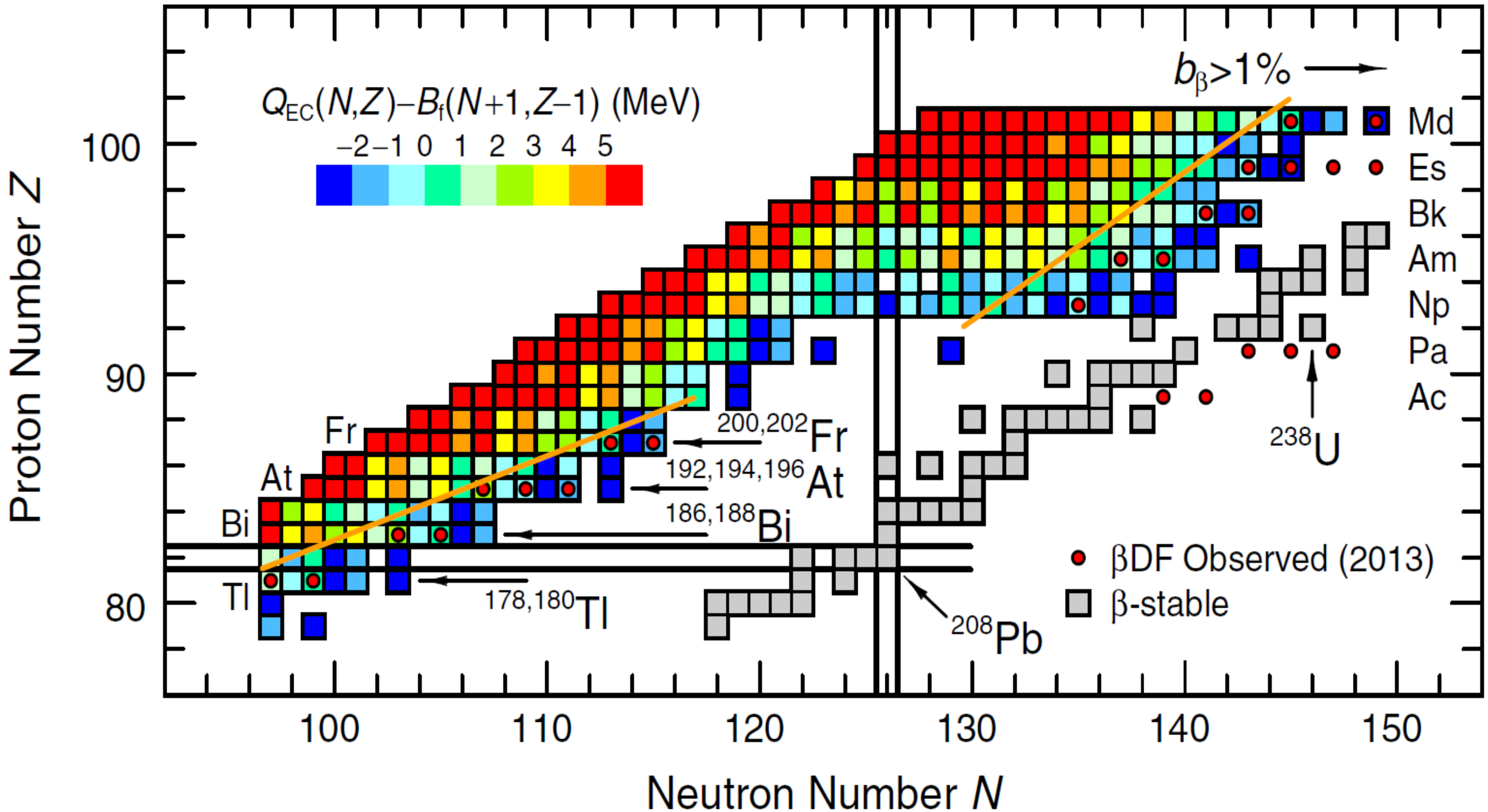

# Low-energy fission

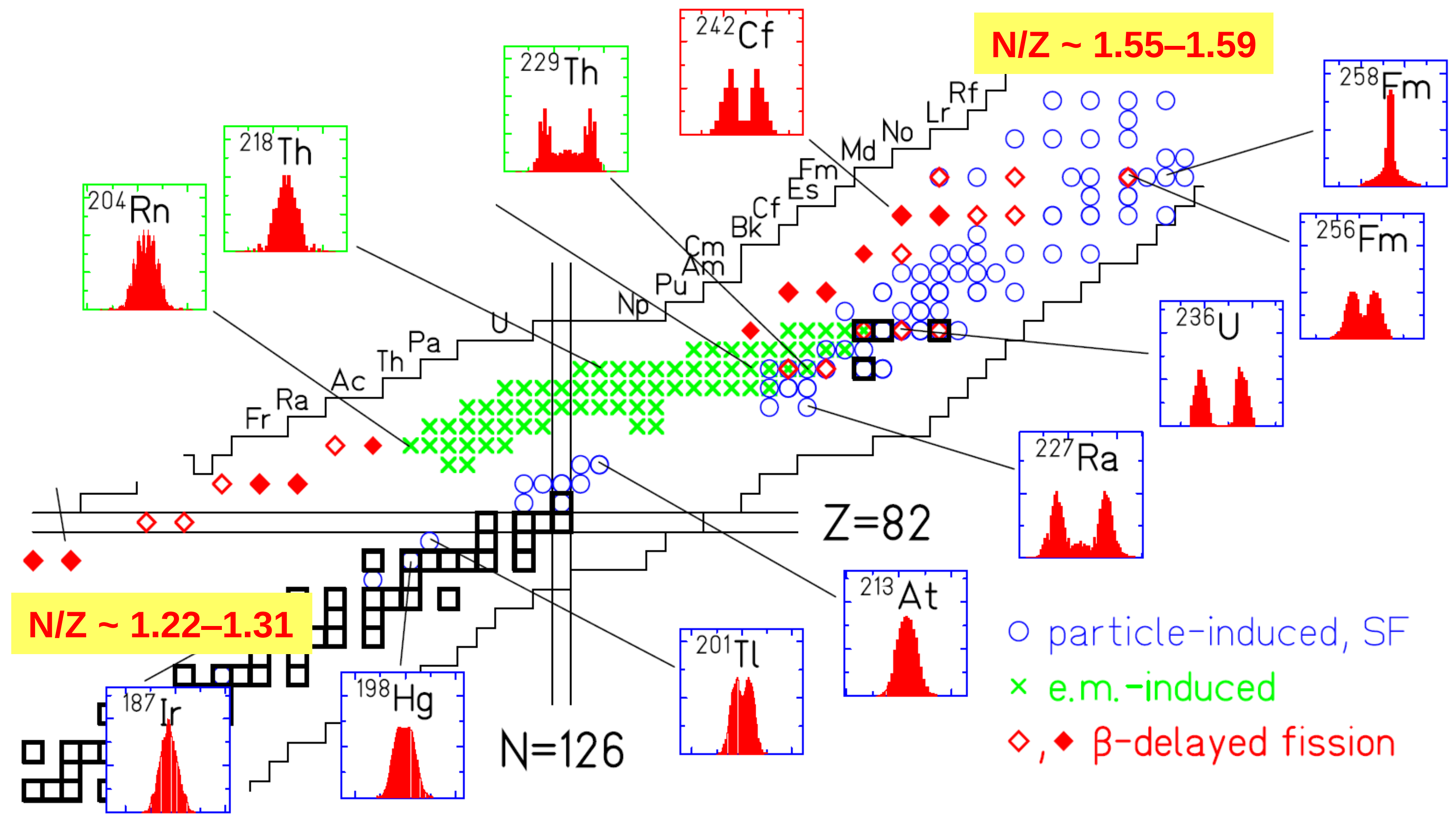


26 βDF isotopes, only 11 with A/Z distribution

# Bimodal fission: $^{258}$Fm, $^{259,260}$Md, $^{258}$No, $^{260}$Rf

E. K. Hulet et al., Phys. Rev. C 40, 770 (1989)

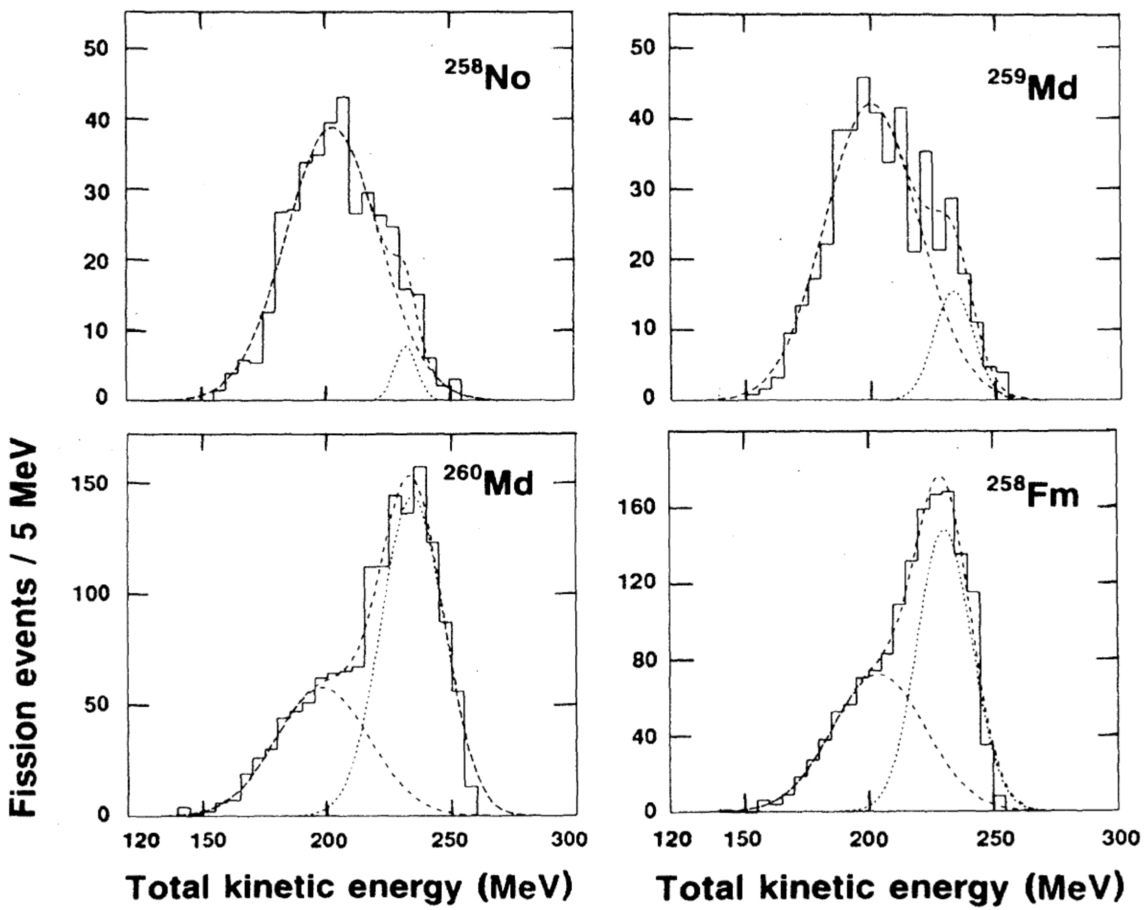


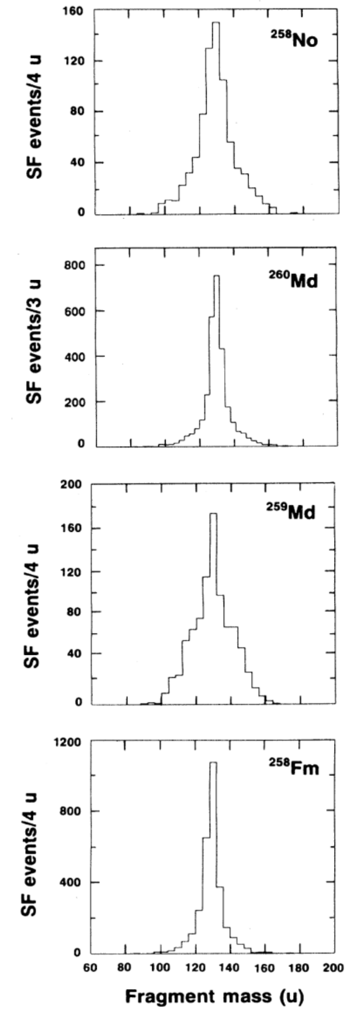


Unfolding of the asymmetric TKE distributions into two Gaussians

# Bimodal fission: $^{258}$Fm, $^{259,260}$Md, $^{258}$No, $^{260}$Rf

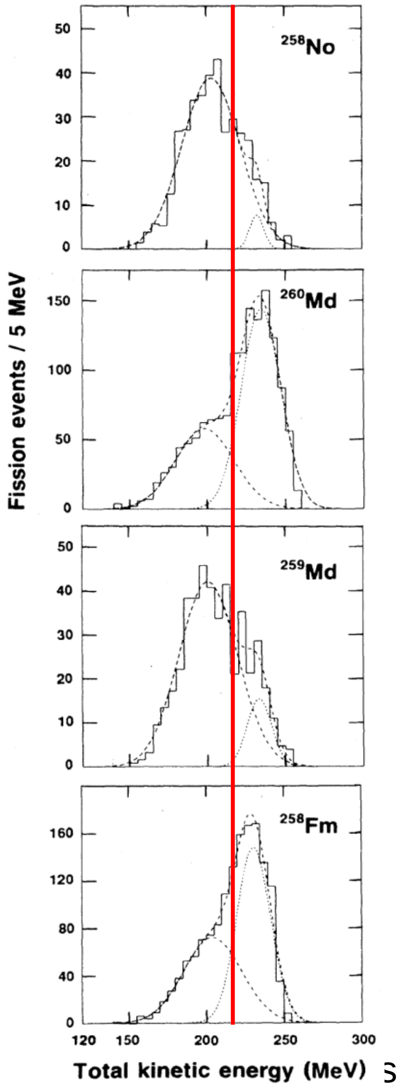


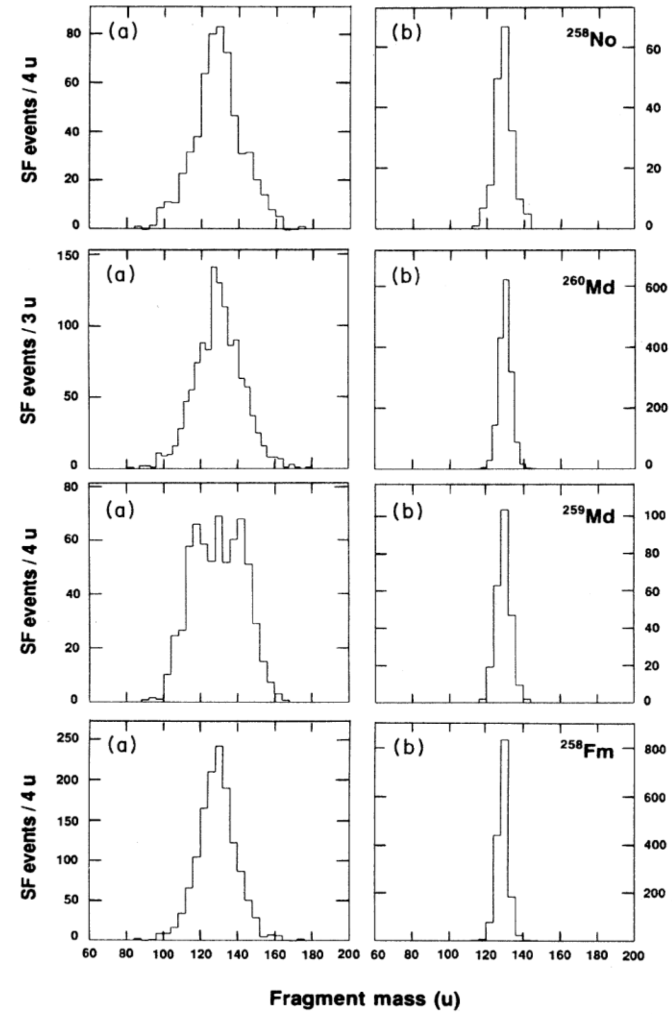


Mass distributions: (a) for events with TKE's<220 MeV and (b) for those with TKE's > 220 MeV

E. K. Hulet et al., Phys. Rev. C 40, 770 (1989)

# Discovery of multimodal fission

$^{226}Ra$+p (11 MeV)

R. C. Jensen and A. W. Fairhall,
Phys. Rev. 109, 942 (1958)

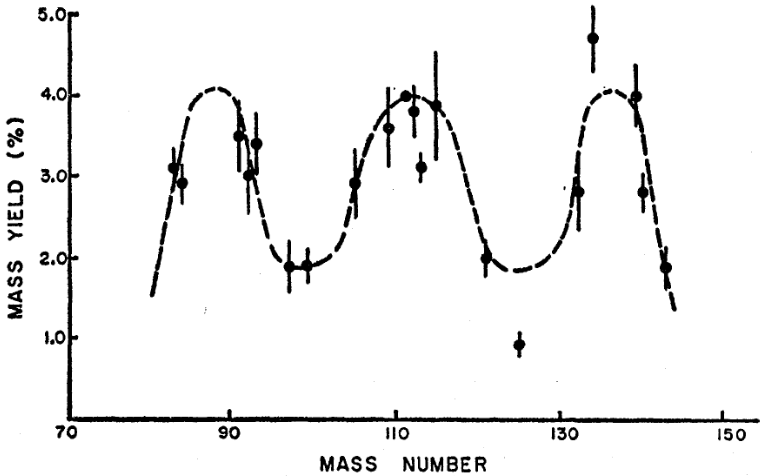


E. Konecny and H. W. Schmitt,
Phys. Rev. 172, 1213 (1968).

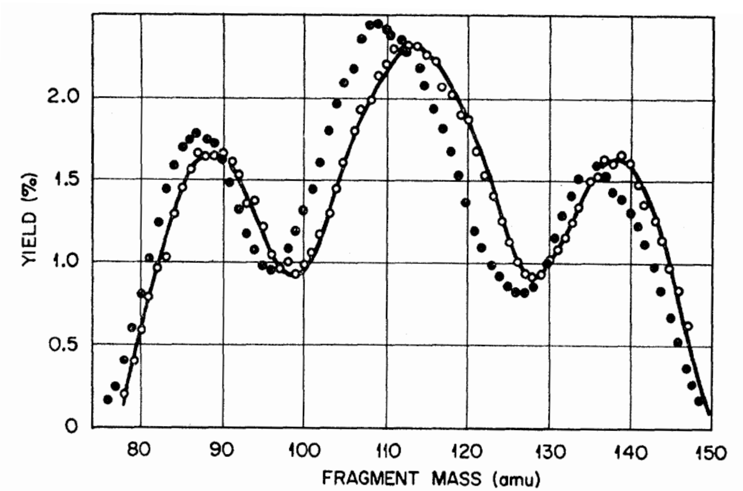


$^{220, 224}Th$:

M.G. Itkis, et al., in: Nuclear Fission and Fission- product Spectroscopy, ILL Grenoble, 1994. pp. 77.

$^{225, 227}Pa$:

I. Nishinaka, et al., Phys. Rev. C 56, 1997. 891

# Multimodal fission: transition from asymmetric to symmetric fission

K.-H. Schmidt, J. Benlliure, and A. R. Junghans, Nucl. Phys. A 693, 169 (2001)

K.-H. Schmidt, et al., Nucl. Phys. A 665, 221 (2000).

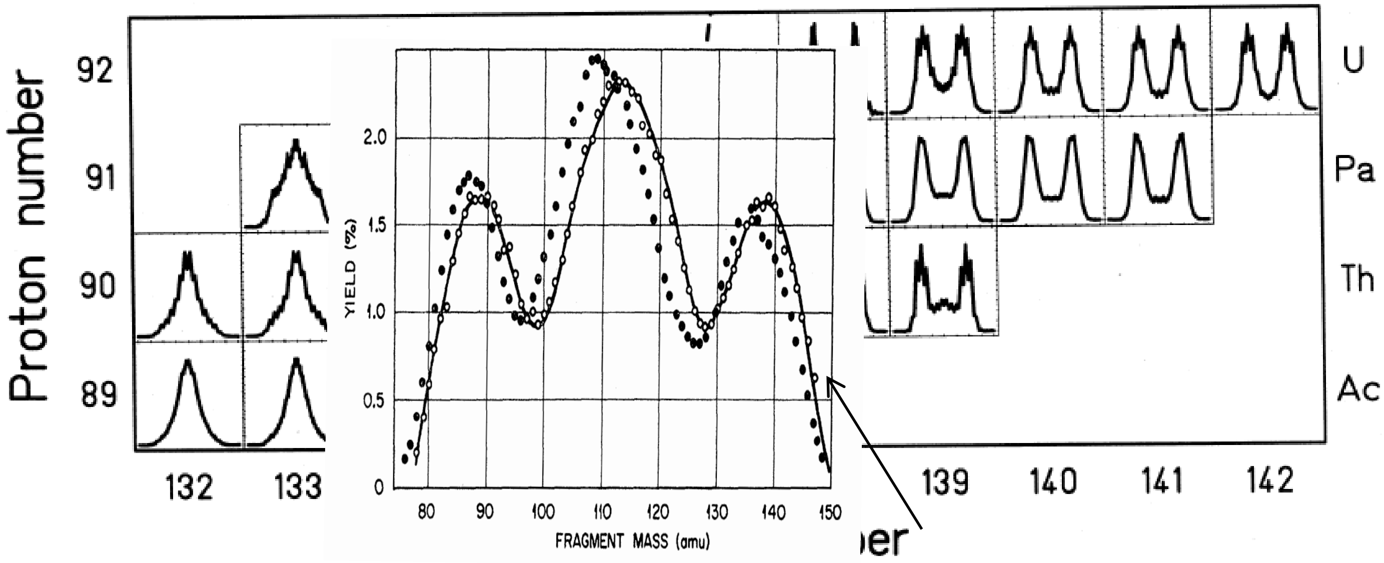


$^{227}$Ac

# Symmetric fission in preactinide and Pb regions

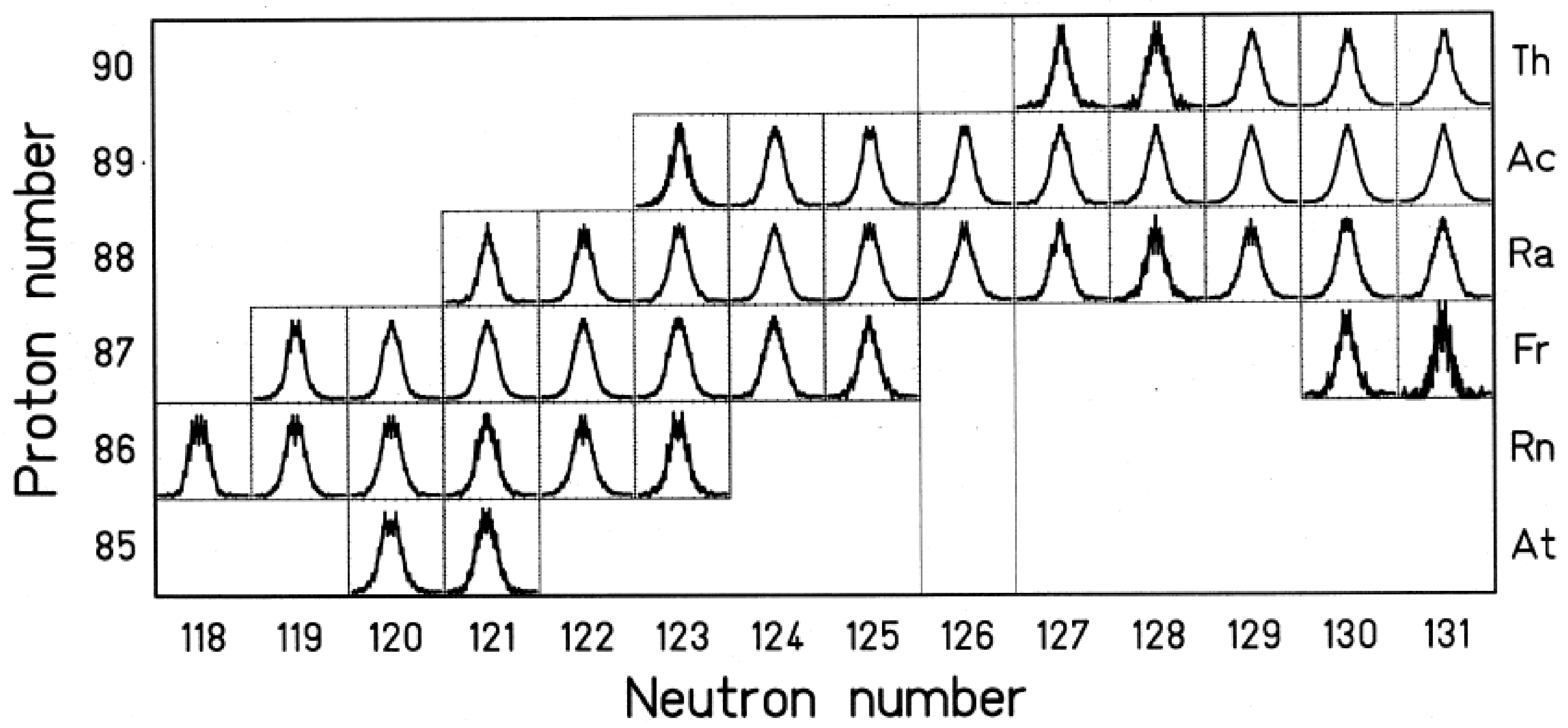


K.-H. Schmidt, J. Benlliure, and A. R. Junghans, Nucl. Phys. A 693, 169 (2001)

K.-H. Schmidt, S. Steinhauser, C. Bockstiegel, A. Grewe, A. Heinz, A. R. Junghans, J. Benlliure, H. G. Clerc, M. de Jong, J. Muller, M. Pfutzner, and B. Voss, Nucl. Phys. A 665, 221 (2000).

# Windmill system at ISOLDE

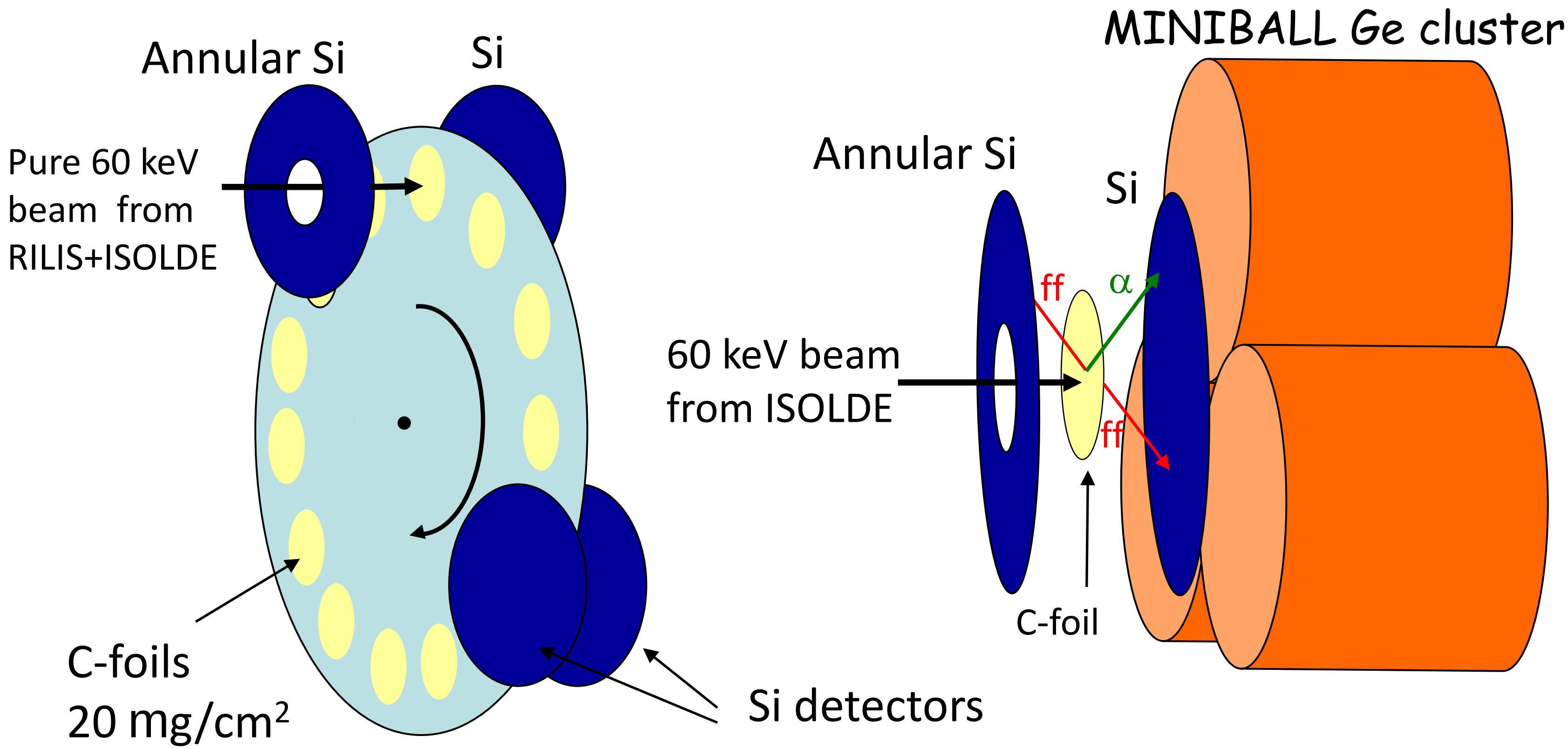


## Setup: Si detectors both sides of the C-foil

- Simple setup & DAQ: 4 PIPS (1 of them – annular)
- Large geometrical efficiency (up to 70%)
- 2 fold fission fragment coincidences (20% efficiency)
- ff-gamma coincidences
- Digital electronics

A.N. Andreyev et al., PRL 105, 252502 (2010)

# ISOLDE: beta-delayed fission

The full-range energy spectrum for $^{196}$At

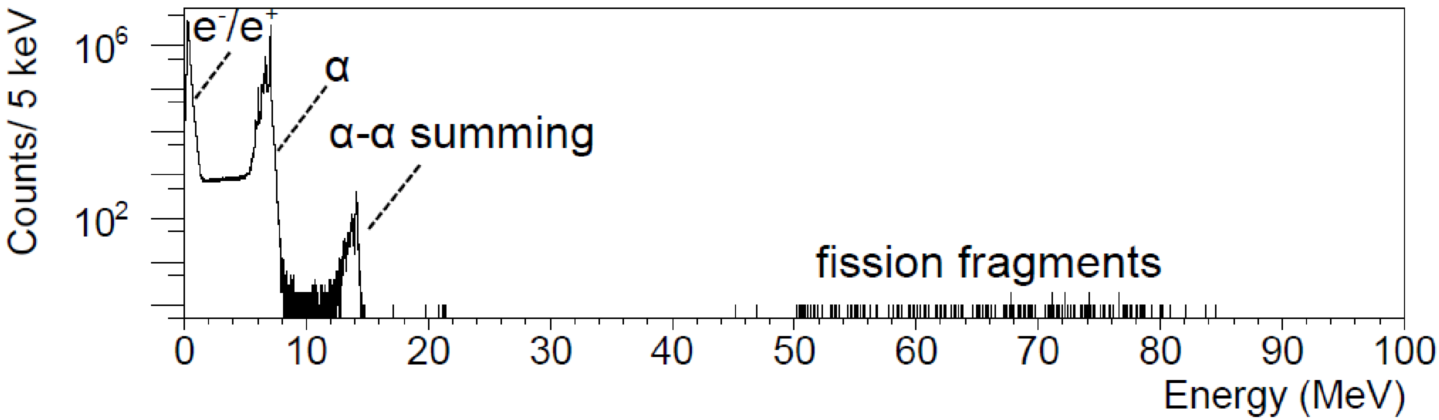


| data set | S FFs | D FFs | $N_\alpha/N_{\beta\mathrm{df}}$ | time |
|---|---|---|---|---|
| $^{194}$At - HRS | 8 | 3 | $2.0^{+17}_{-8} \times 10^3$ | 1h 13m |
| $^{194}$At - GPS | 385 | 106 | $1.7(1) \times 10^3$ | 9h 11m |
| $^{196}$At - HRS | 14 | 5 | $3.9^{+19}_{-12} \times 10^5$ | 5h 25m |
| $^{196}$At - GPS | 273 | 68 | $4.3(5) \times 10^5$ | 35h 7m |
| $^{200}$Fr - HRS | 1 | 0 | $2.5^{+123}_{-17} \times 10^3$ | 21h 34m |
| $^{200}$Fr - GPS | 7 | 2 | $1.5^{+12}_{-6} \times 10^3$ | 20h 18m |
| $^{202}$Fr - HRS | 115 | 43 | $1.4(2) \times 10^4$ | 43h 59m |

# ISOLDE: beta-delayed fission

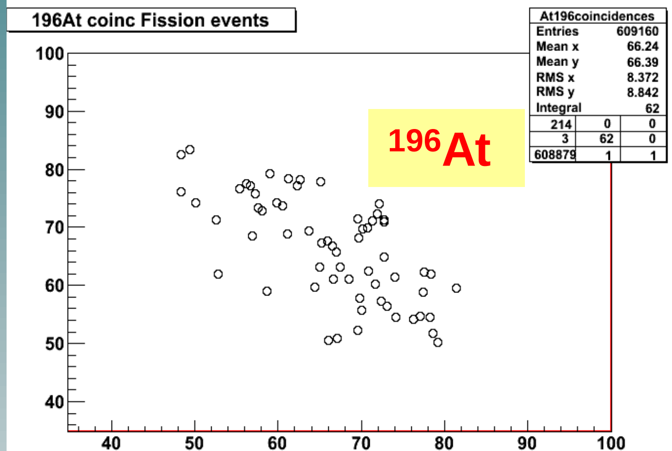


Clear di... mass ... fissio ... rgy (thus, ... etween ... 194,196Po

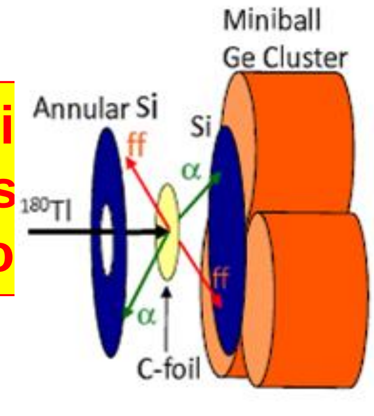


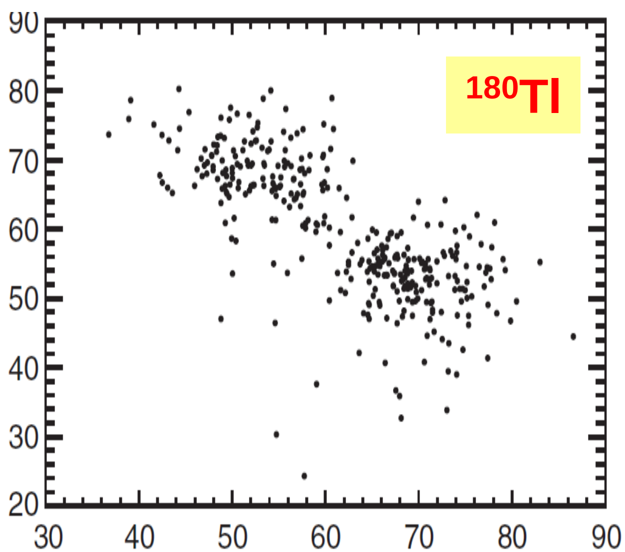


Energy in Si2 (MeV)

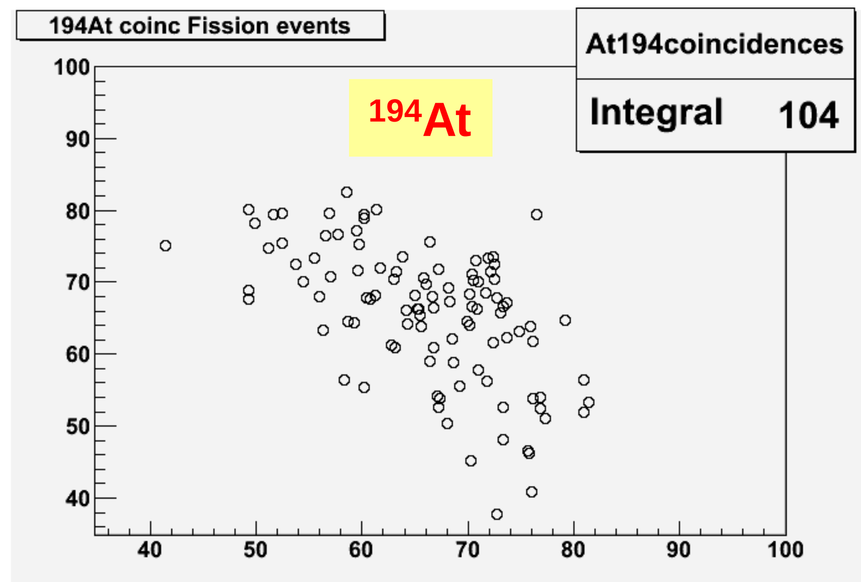


Energy in Si1 (MeV)

# ISOLDE: beta-delayed fission

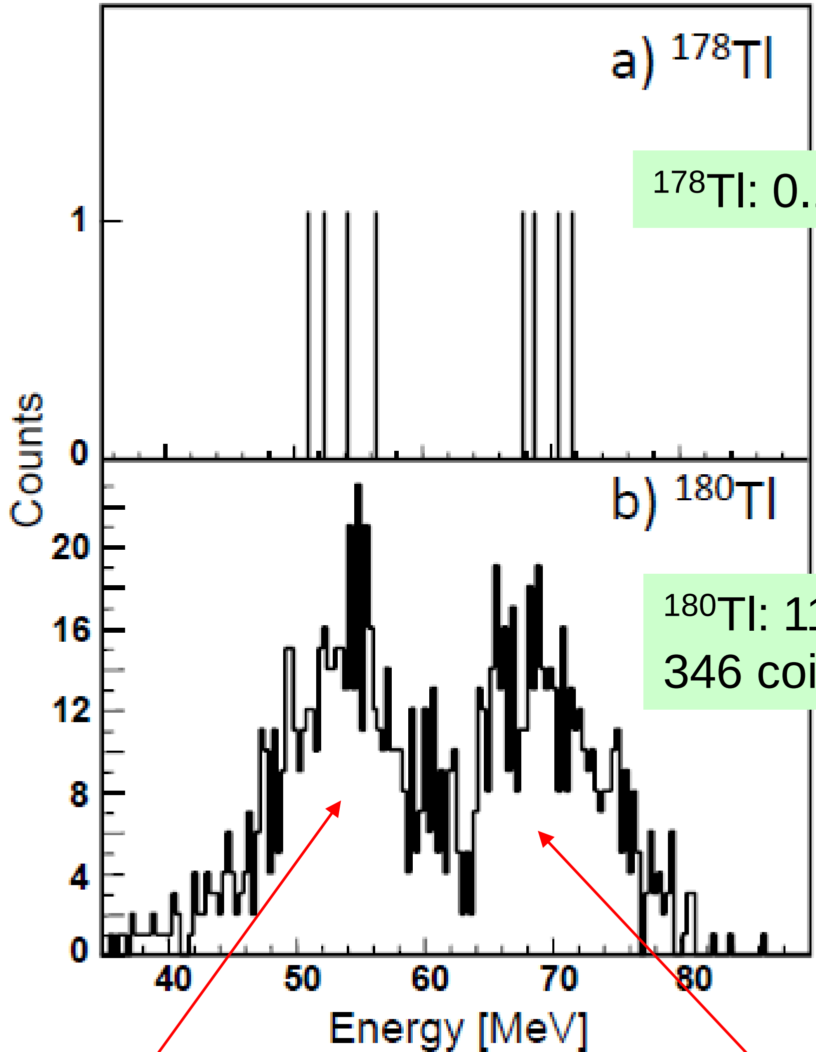


$^{178}$Tl: 0.1 ions/μC/s, 8 fission events

$P_{\beta DF}$ ($^{178}$Tl)=0.15(6)%

$^{180}$Tl: 1111 fission events,
346 coincidence events

$P_{\beta DF}$ ($^{180}$Tl)=3.2(2)×10$^{-3}$%

corresponds to A=80(1)

FWHM ≈ 9 amu

A=100(1)

# New type of asymmetric fission

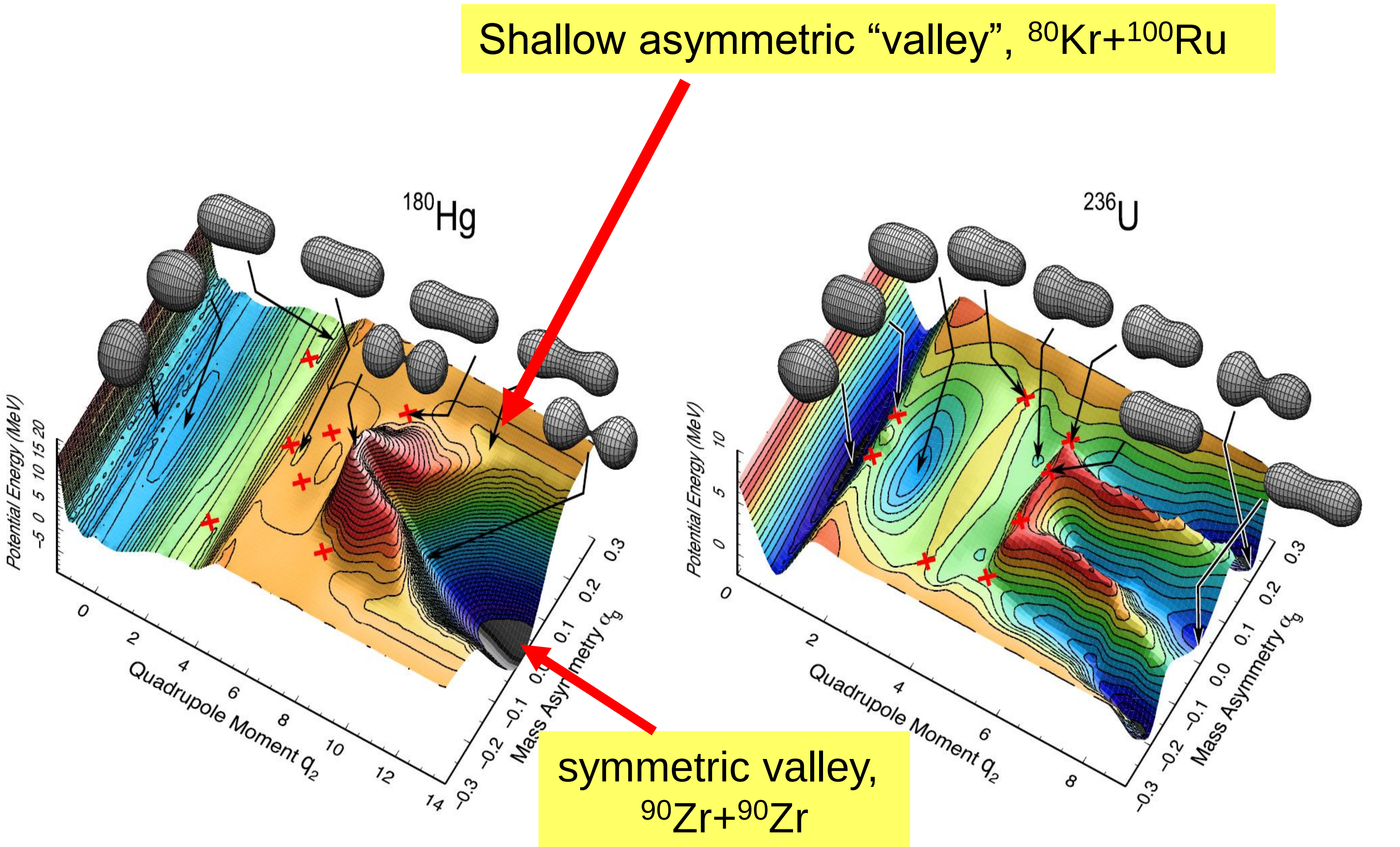


competition between symmetric and asymmetric fission paths

# Fragment mass distribution in βDF of Tl isotopes (theory)

**1. Model: BSM(M)**

Brownian shape motion on five-dimensional (5D) potential energy surfaces in Metropolis random-walk approximation

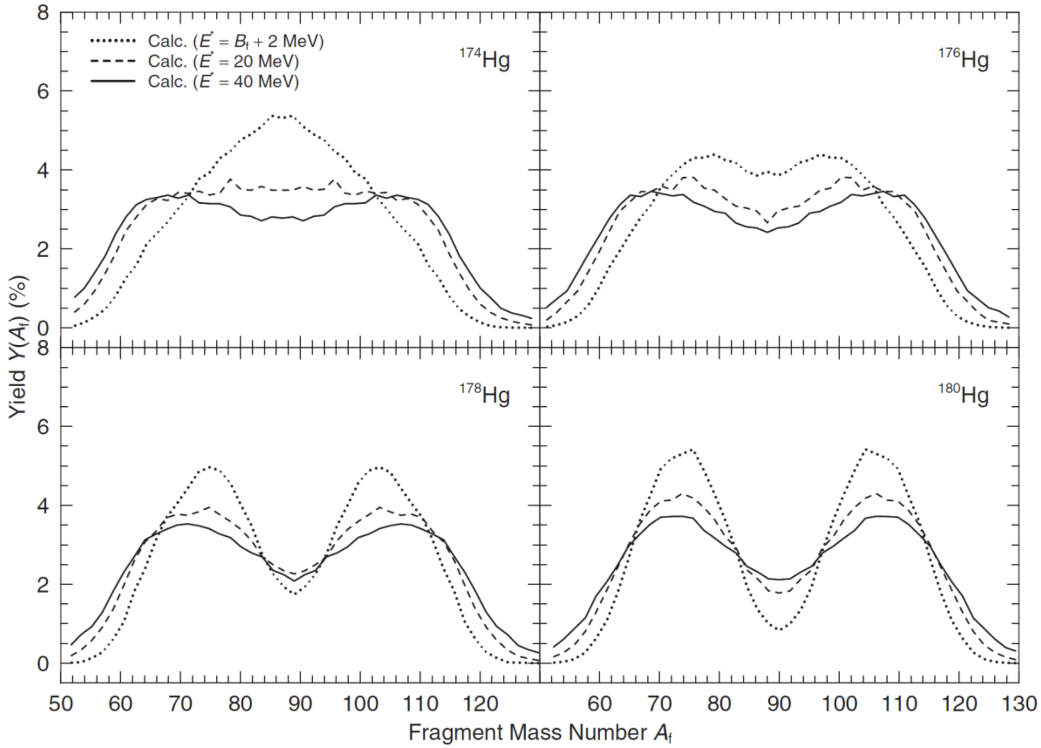


Calculated yields for four Hg isotopes at three excitation energies.
For the lighter isotopes the yields become more symmetric.

P. Möller, J. Randrup, A. Sierk, Phys. Rev. C **85**, 024306 (2012)

M. Veselsky *et al*. Phys. Rev. C **86**, 024308 (2012)

# Fragment mass distribution in βDF of Tl isotopes (theory)

2. HF calculations (SkM* and D1S forces) predict the similar PES for $^{180}$Hg with $A_H/A_L$=99/81 at asymmetric scission point and very soft in $Q_{30}$ direction PES for $^{198}$Hg

Warda, M., A. Staszczak, and W. Nazarewicz, 2012, Phys. Rev. C86, 024601

3. "Scission point" model (assumption that statistical equilibrium is established at scission and the observable characteristics of the fission process are formed near the prescission configurations)

Andreev, A.V., G.G. Adamian, and N.V. Antonenko, 2012, Phys. Rev. C 86, 044315

3a. HF-based "scission point" model

Panebianco, S., J.-L. Sida, H. Goutte, J.-F. Lemaître, N. Dubray, and S. Hilaire, 2012, Phys. Rev. C 86, 064601

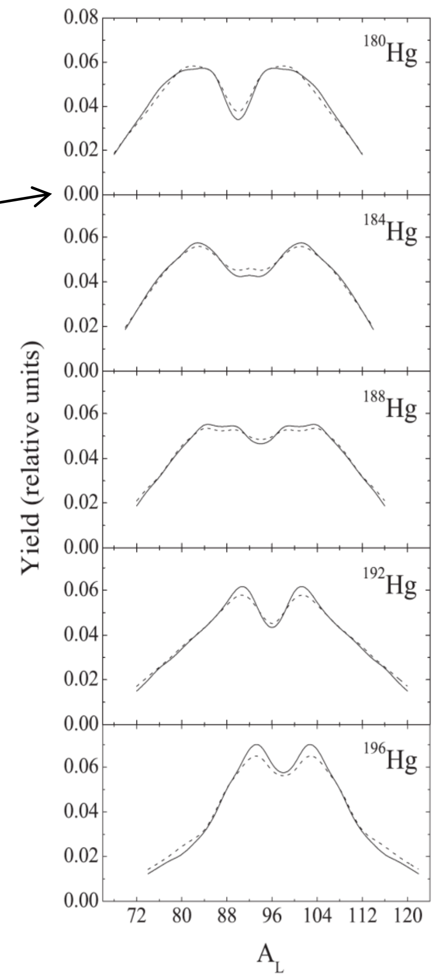

# Fission barriers for Hg isotopes (comparison with theory)

$$P_{\beta DF} = \frac{N_{\beta DF}}{N_\beta} = \frac{\int_0^{Q_\beta} F(Q_\beta - E) S_\beta(E) \Gamma_f(E)/\Gamma_{total}(E) dE}{\int_0^{Q_\beta} F(Q_\beta - E) S_\beta(E) dE}$$

$$\Gamma_f(E^*) = \frac{1}{2\pi \rho_c(E^* - \Delta)} \int_0^{E^* - B_f - \Delta_{sp}} \rho_{sp}(E^* - B_f - \Delta_{sp} - E') dE'$$

| | $B_f$, exp (model), MeV | $B_f$, theor MeV |
|---|---|---|
| $^{180}$Hg | 7.5(1.5) | 9.8 |
| $^{178}$Hg | ~ 7 | 9.3 |

Fission barriers deduced from the βDF studies in the lead region confirm an earlier inference on the reduced fission barriers obtained from data on cross sections of heavy ion reactions

$P_{\beta DF}$ $(^{180}Tl)_{theor}$= $2\times10^{-6}$%
$P_{\beta DF}$ $(^{180}Tl)_{exp}$= $3.2(2)\times10^{-3}$%

# Beta-delayed fission: partial half-life

$$T_{1/2p,\beta\mathrm{DF}} = \frac{T_{1/2,\mathrm{tot}}}{b_\beta P_{\beta\mathrm{DF}}} \xrightarrow{b_\beta \leq 10\%} T_{1/2p,\beta\mathrm{DF}} \simeq T_{1/2,\mathrm{tot}}(N_\alpha / N_{\beta\mathrm{DF}})$$

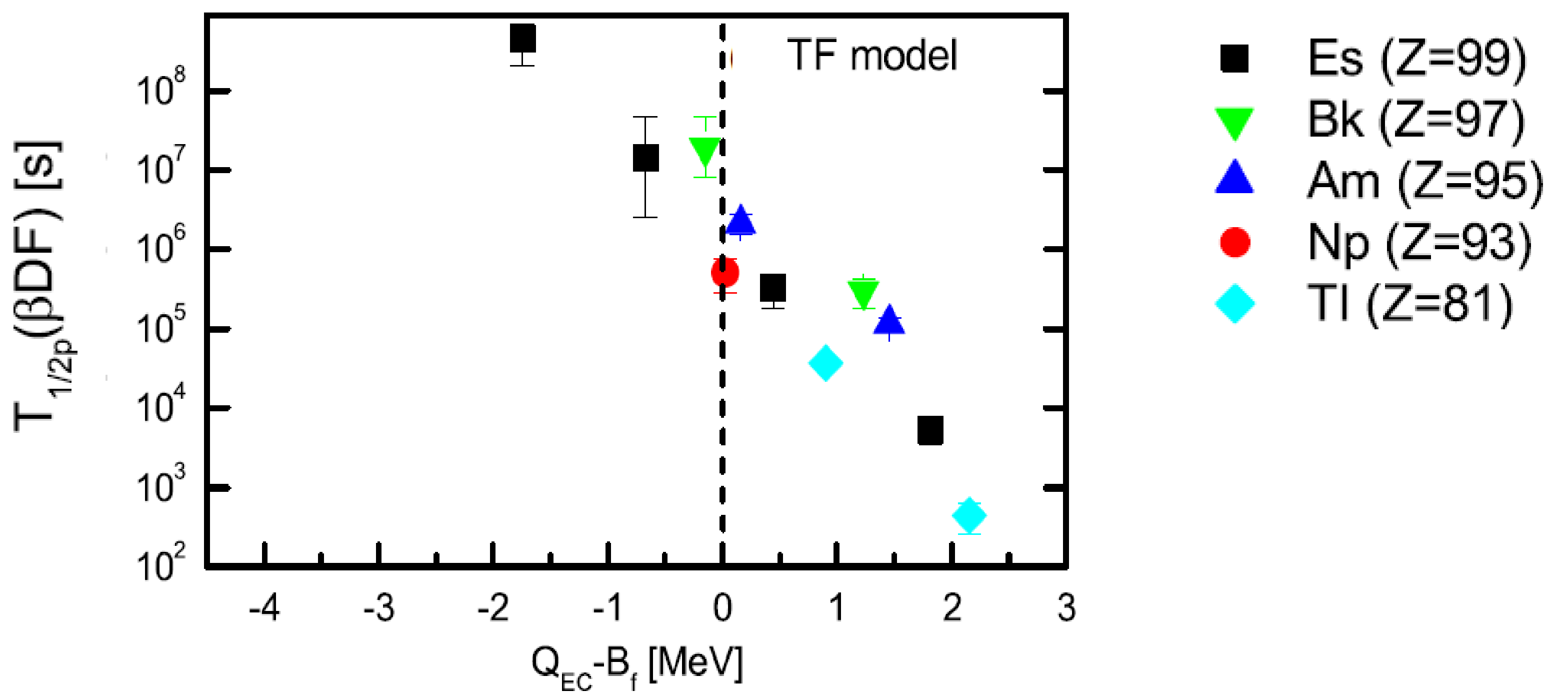


Systematics of βDf partial half-lives vs. $Q_\beta$-$B_f$ points to some universal law

# Low-energy fission: comparison with theory

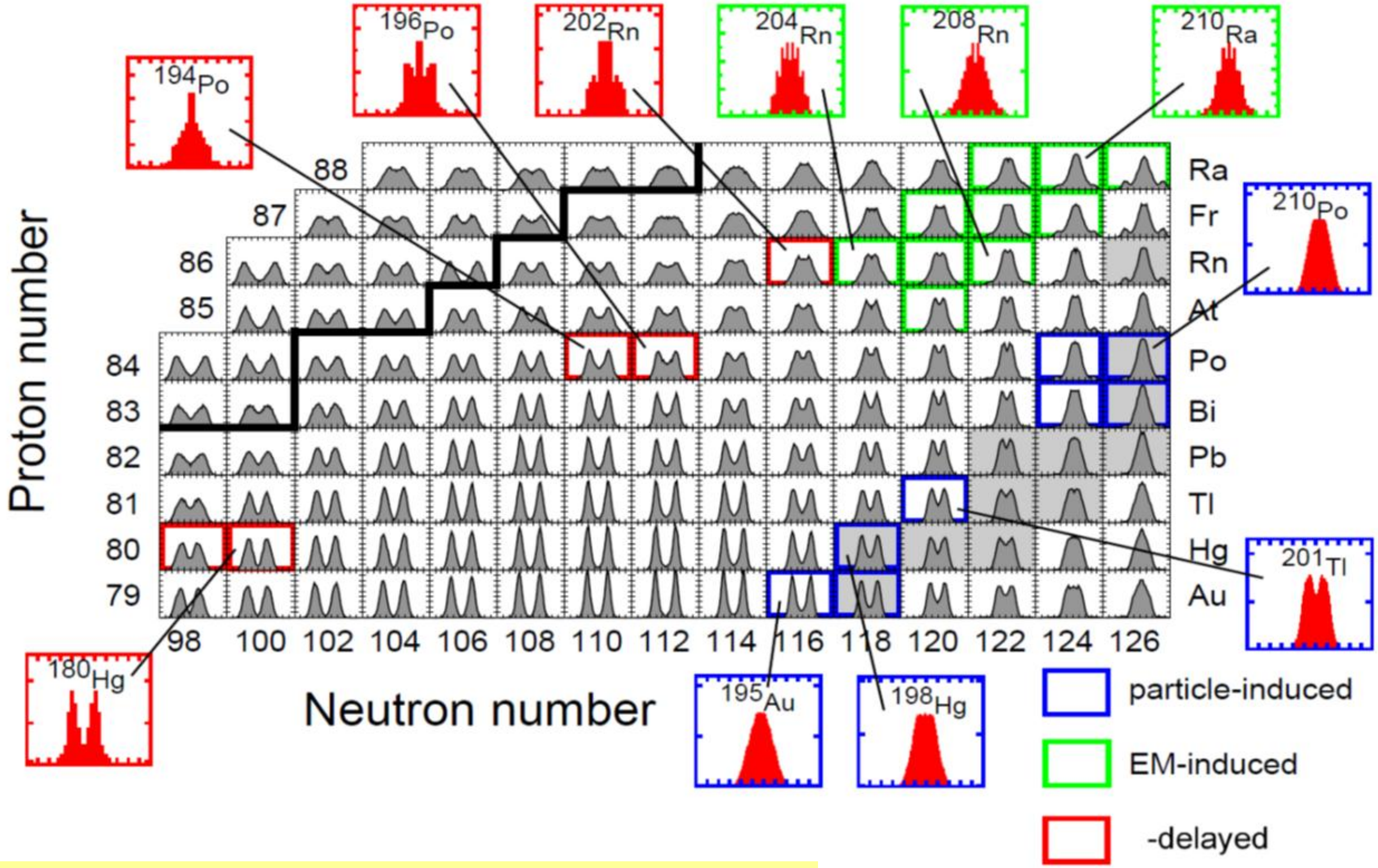


J. Randrup, P. Möller, Phys. Rev. C **88**, 064606 (2013).

P. Möller, J. Randrup, A. Sierk, Phys. Rev. C **85**, 024306 (2012)

M. Veselsky *et al*. Phys. Rev. C **86**, 024308 (2012)

# ISOLDE: beta-delayed fission

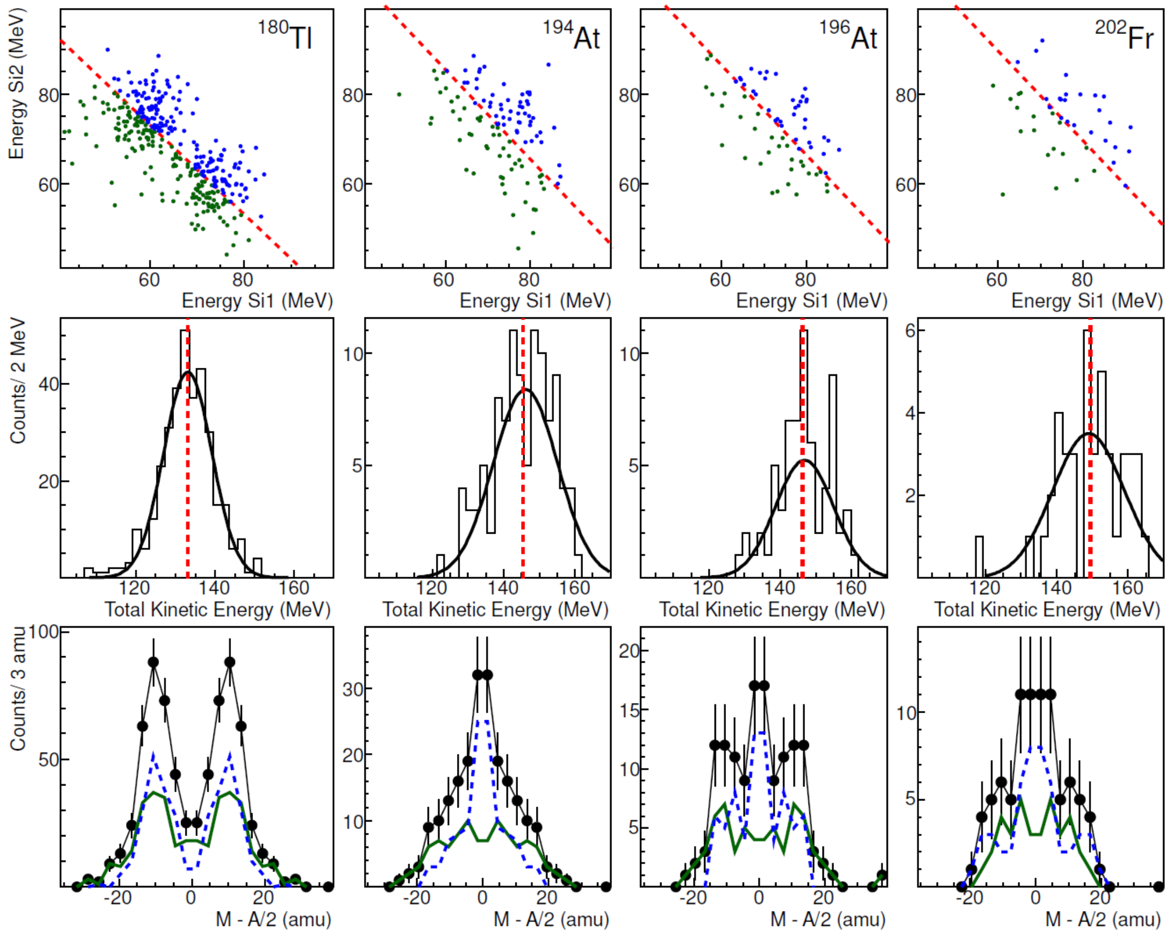


energy distribution of coincident FFs

total kinetic energy

mass distributions

$P_{\beta DF}$ ($^{196}$At)=9(1) ×$10^{-3}$

$P_{\beta DF}$ ($^{194}$At) and $P_{\beta DF}$ ($^{202}$Fr) can't be determined due to the presence of isomers

# ISOLDE: isomer-selective βDf

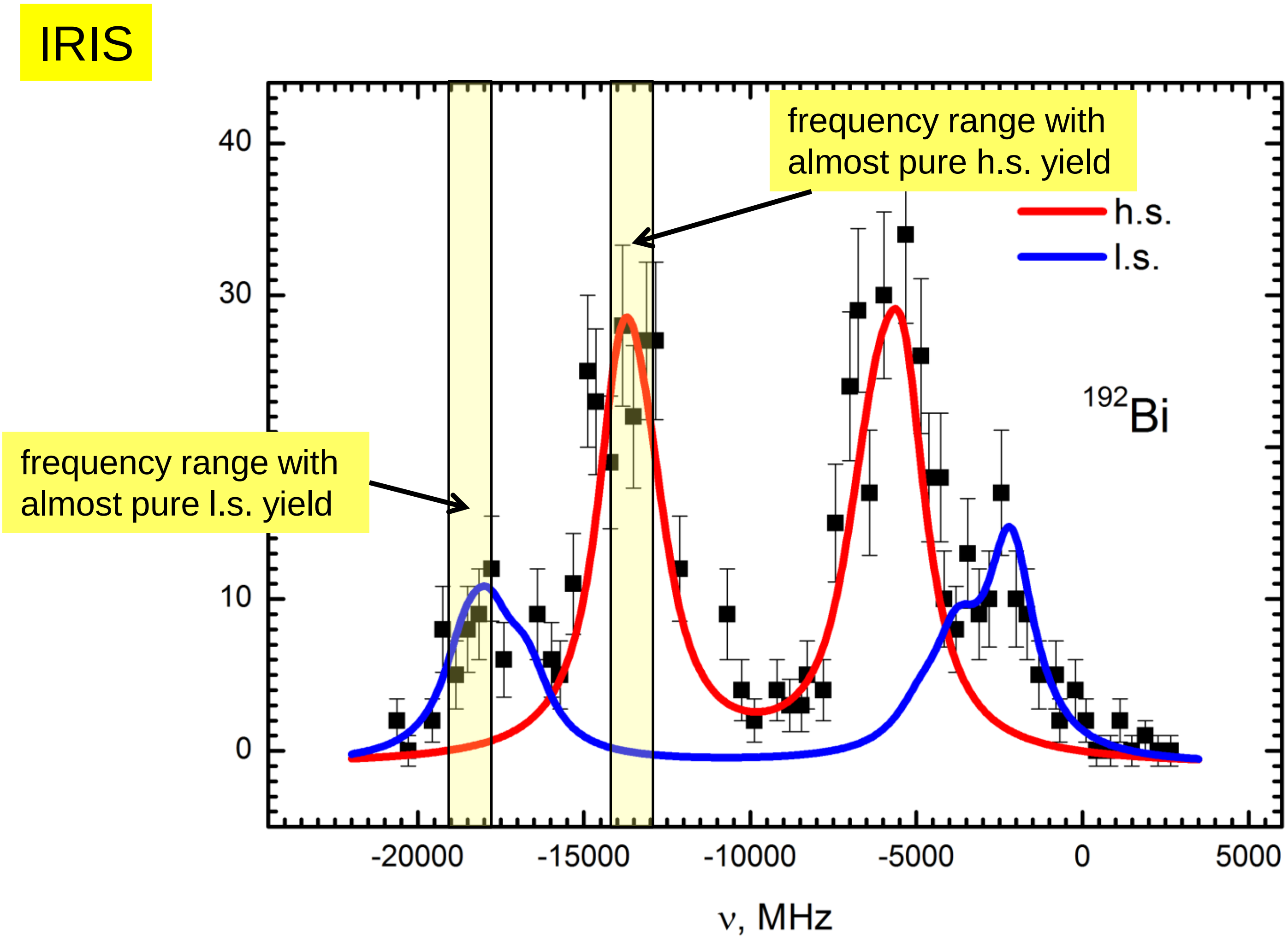

# ISOLDE: isomer-selective βDf

Hyperfine structure study of $^{194}At^{g,m}$
to enable isomer-selective βDf measurements

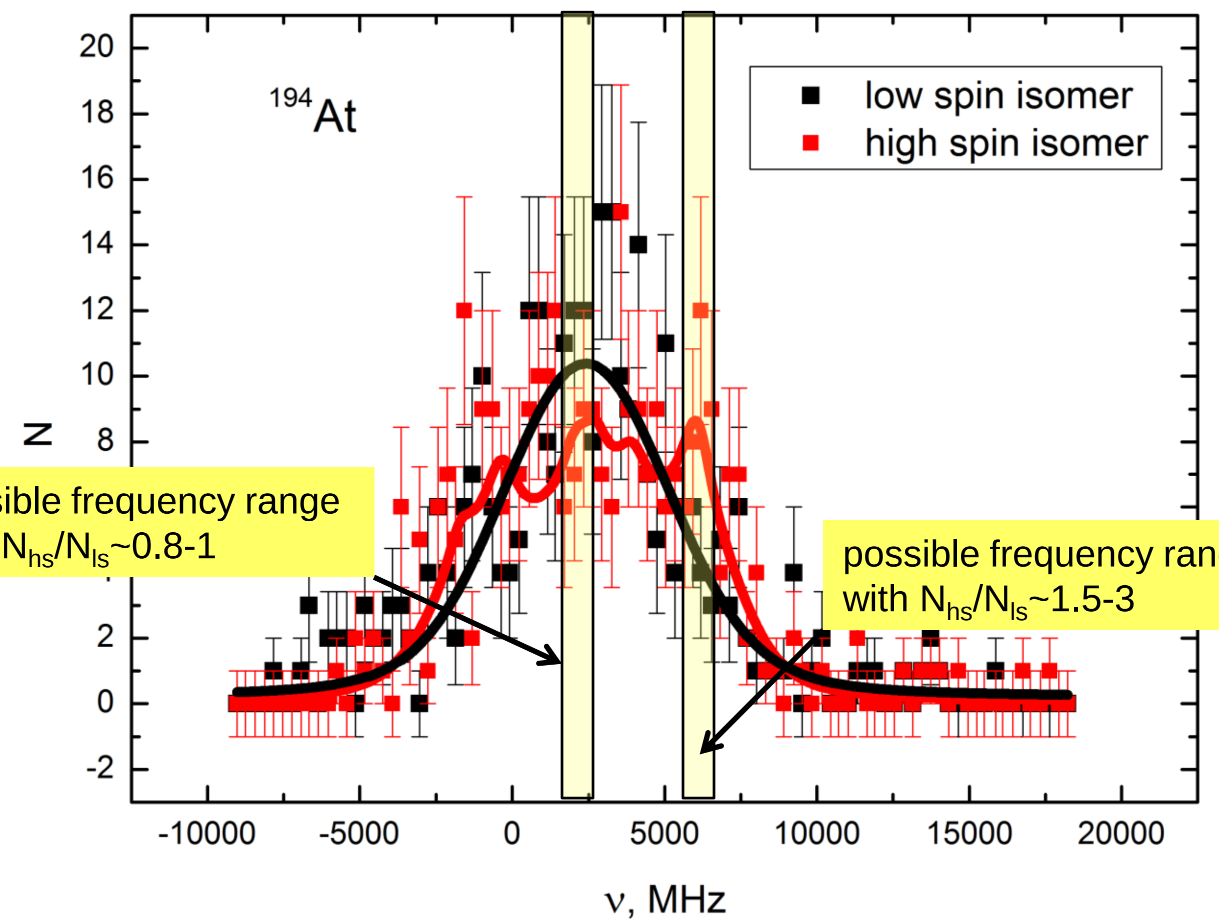


possible frequency range with $N_{hs}/N_{ls}$~0.8-1

possible frequency range with $N_{hs}/N_{ls}$~1.5-3

# ISOLDE: beta-delayed fission

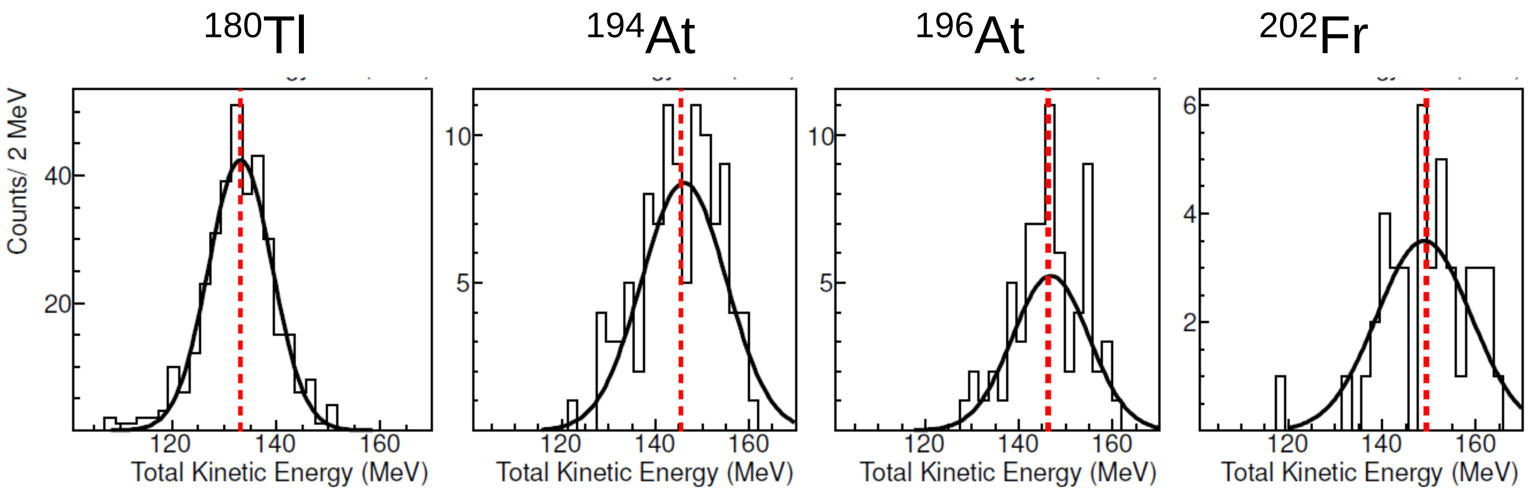


| | $\overline{\mathrm{TKE}}$ (MeV) | $\sigma$ (MeV) | $A_L$ | $\Delta A/A_{tot}$ |
|---|---|---|---|---|
| $^{180}\mathrm{Tl} \xrightarrow{\beta} {}^{180}\mathrm{Hg}$ (ff) | 133.1(3) | 6.1(3) | 80(1) | 0.11(1) |
| $^{194}\mathrm{At} \xrightarrow{\beta} {}^{194}\mathrm{Po}$ (ff) | 146(1) | 9.0(13) | - | - |
| $^{196}\mathrm{At} \xrightarrow{\beta} {}^{196}\mathrm{Po}$ (ff) | 147(1) | 8.1(15) | 88(2) | 0.10(2) |
| $^{202}\mathrm{Fr} \xrightarrow{\beta} {}^{202}\mathrm{Rn}$ (ff) | 149(2) | 10(3) | 89(2) | 0.12(2) |

TKE distribution in triple-humped cases ($^{194,196}$At, $^{202}$Fr) is markedly broader than in pure asymmetric case ($^{180}$Tl), whereas the mass split is the same

# ISOLDE: correlation between TKE and fission mode

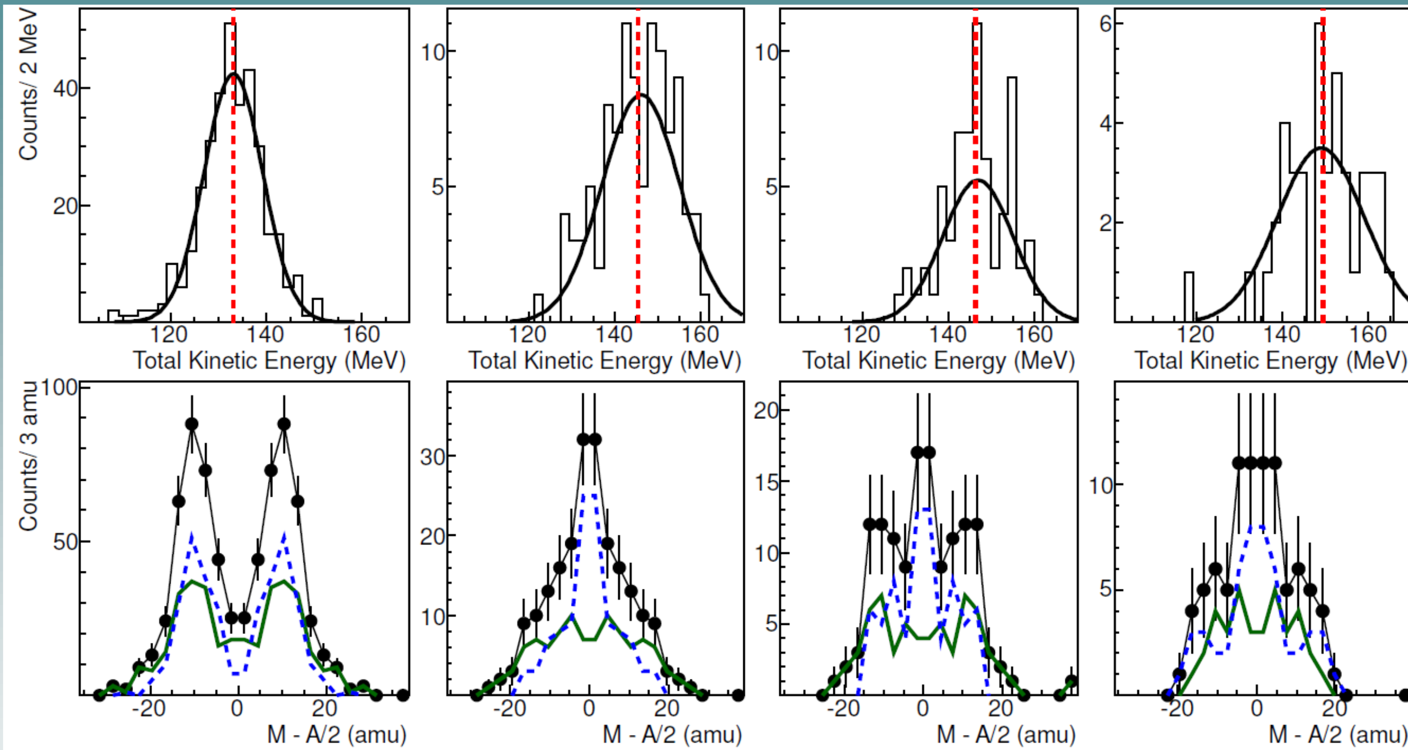


$^{180}$Tl $^{194}$At $^{196}$At $^{202}$Fr

The green and blue curves represent data below and above the average TKE (red dashed lines in top figure):
Higher energy events favor asymmetric mode, lower energy events – symmetric mode…

# Correlation between TKE and fission mode: $^{227}$Ac

…it is coincide with the conclusion for $^{226}$Ra (p,f) reaction

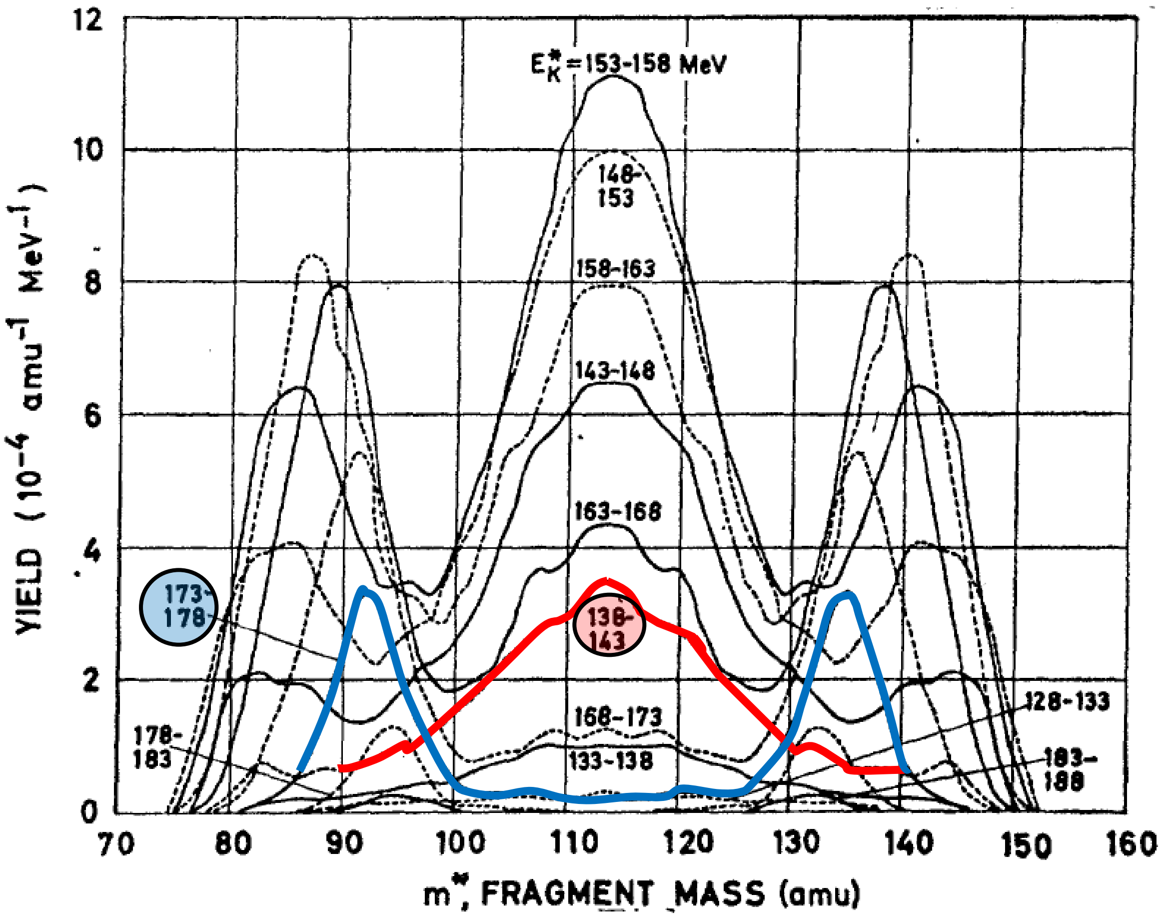


E. Konecny and H. W. Schmitt, Phys. Rev. 172, 1213 (1968).

# PES for $^{196}$Po: different fission paths

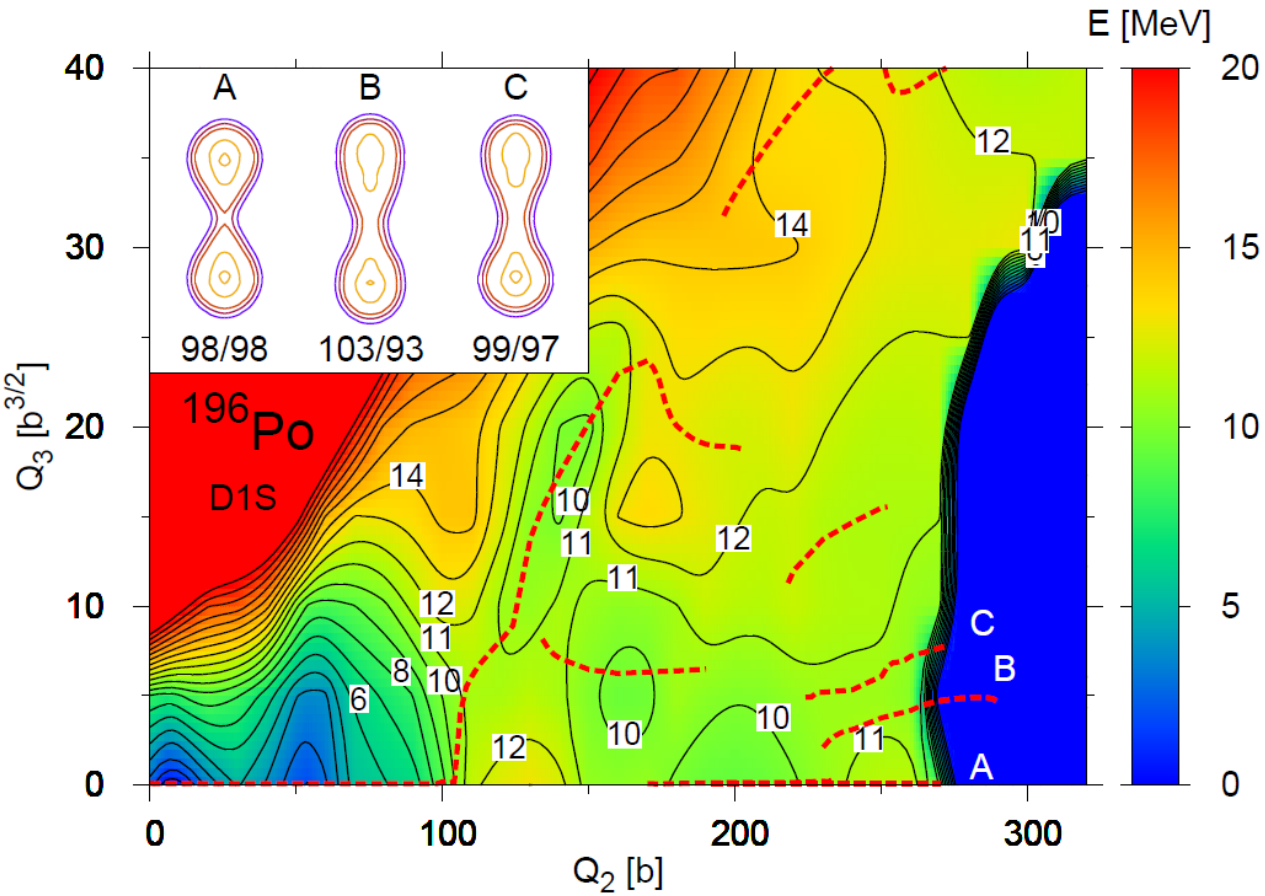


Calculated PES for $^{196}$Po from a microscopic HFB theory. Dashed lines represent fission paths.

# Transition from asymmetric to symmetric fission

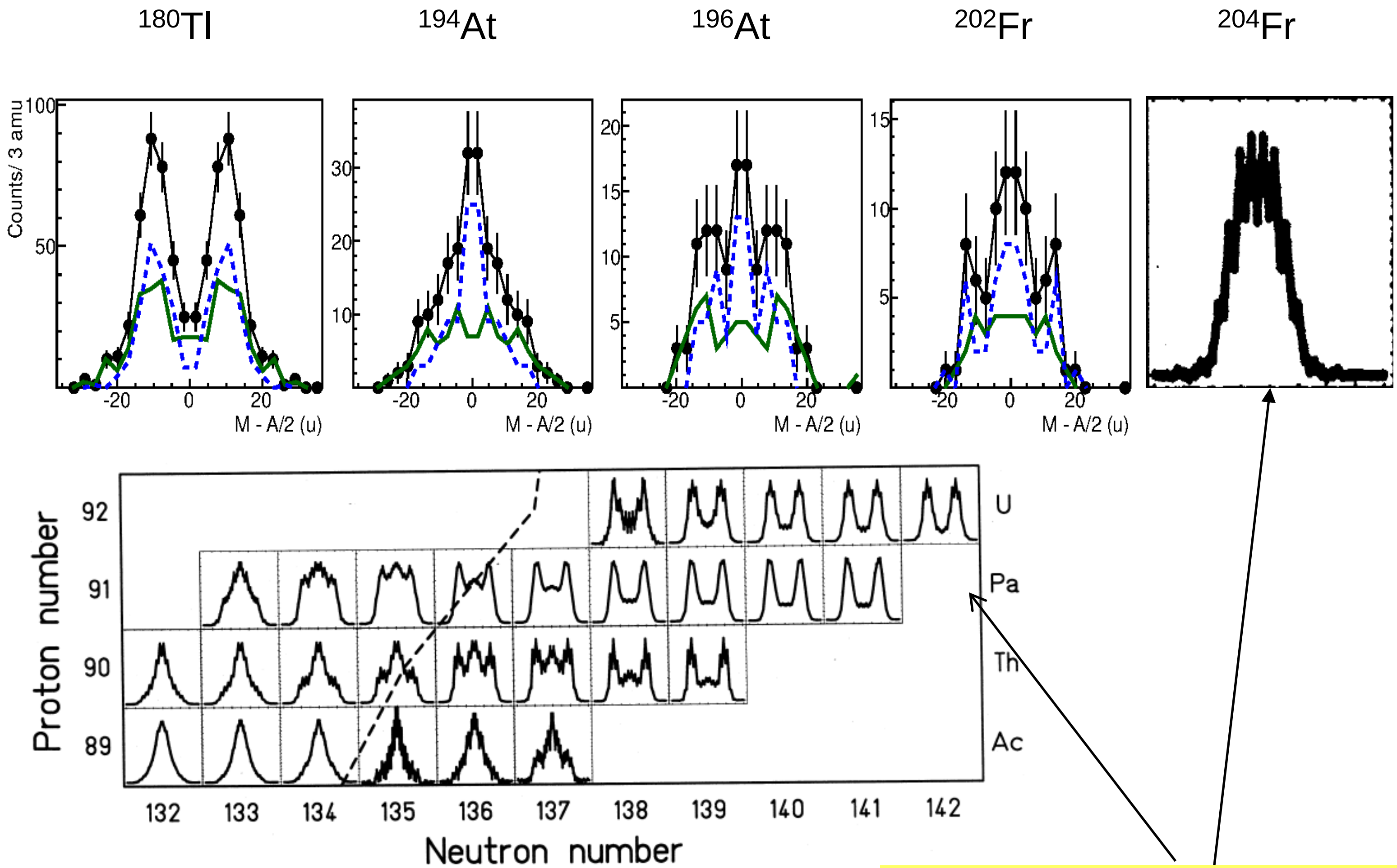


K.-H. Schmidt et al., Nucl. Phys. A 665, 221 (2000)

transition from asymmetric to symmetric fission through multimodal region

# Transition from asymmetric to symmetric fission

ISOLDE

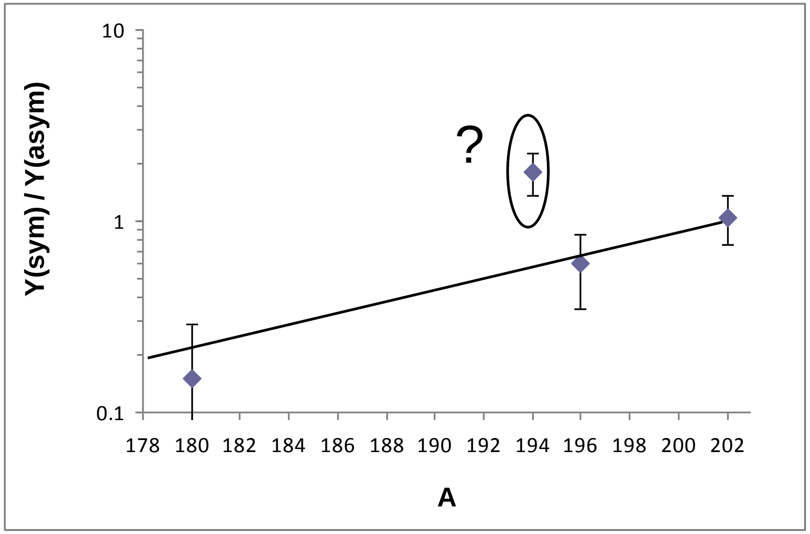


Intensity ratios of the symmetric and the asymmetric fission components in the transitional region as a function of mass number

GSI

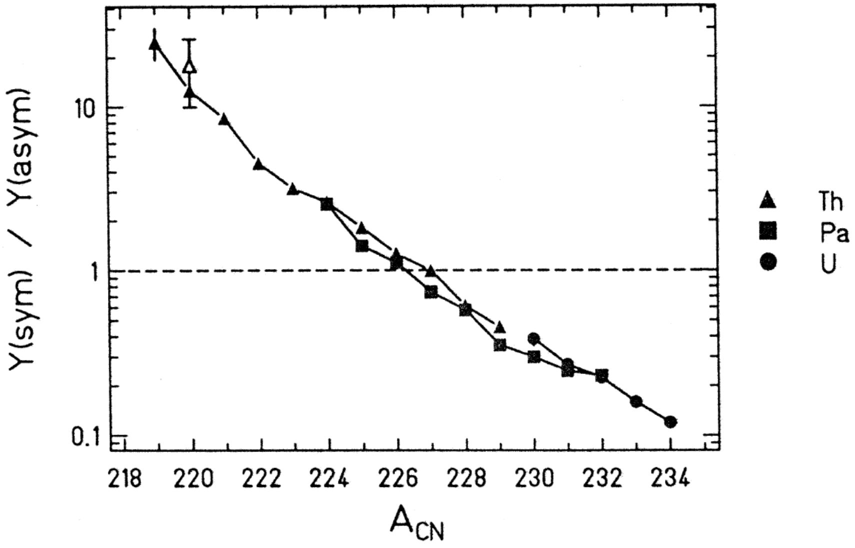

# Transition from asymmetric to symmetric fission

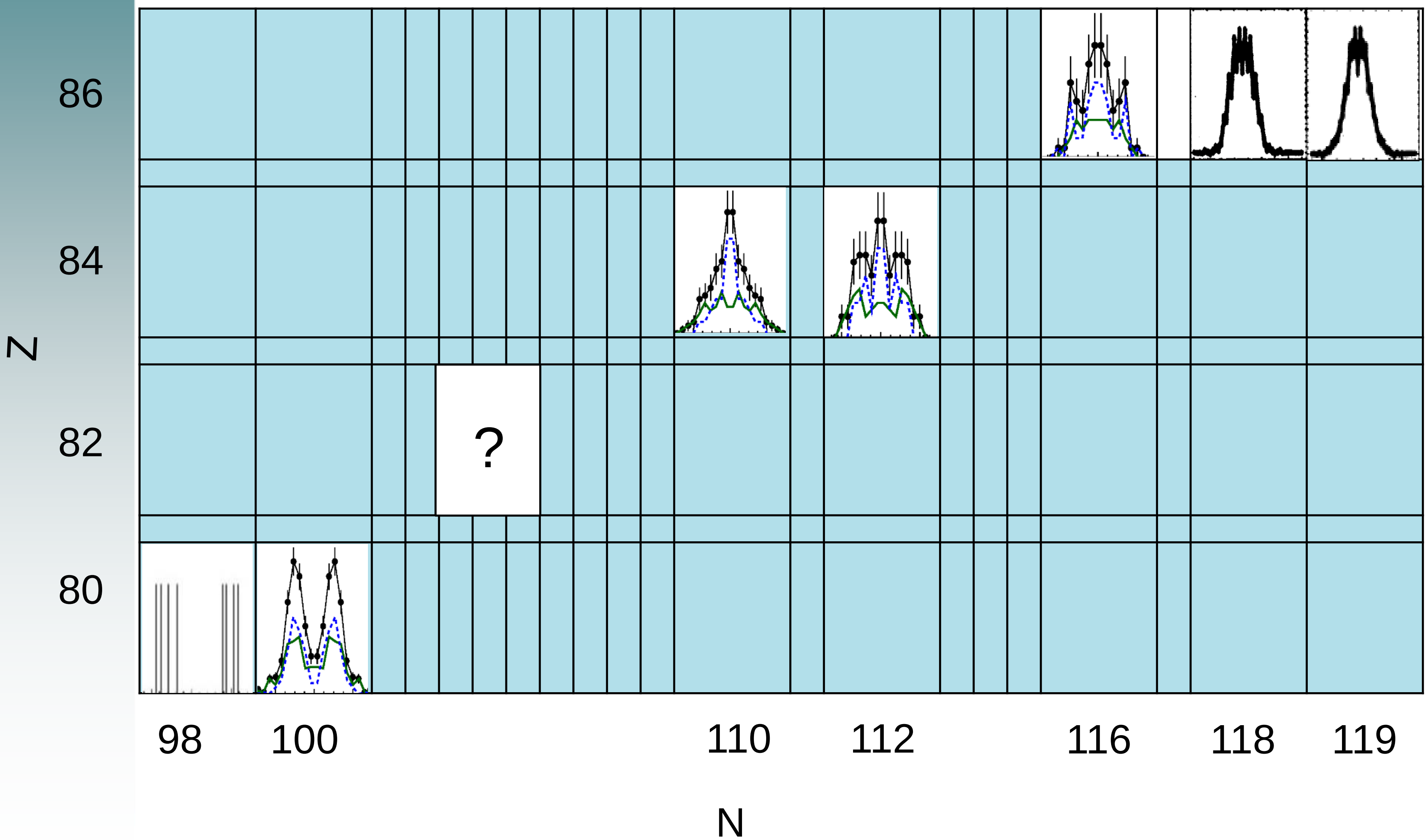

# ISOLDE: βDF— conclusions and outlook

1. Измерено массовое распределение осколков в запаздывающем делении $^{194,196}At$ и $^{202}Fr$. Установлено, что переход от асимметричного к симметричному делению в области нейтронно-дефицитных ядер в районе свинца осуществляется через область мультимодального деления. Массовые распределения и вероятности βDF (барьеры деления) не описываются в рамках современных теоретических подходов.

2. Планируется продолжение исследований: βDF для $^{186-190}Bi$, $^{176}Au$; изомерно селективные измерения для $^{194}At$ и $^{202}Fr$; βDF в нейтронно-избыточной области ($^{228-232}Fr$, $^{228-232}Ac$; r-process).

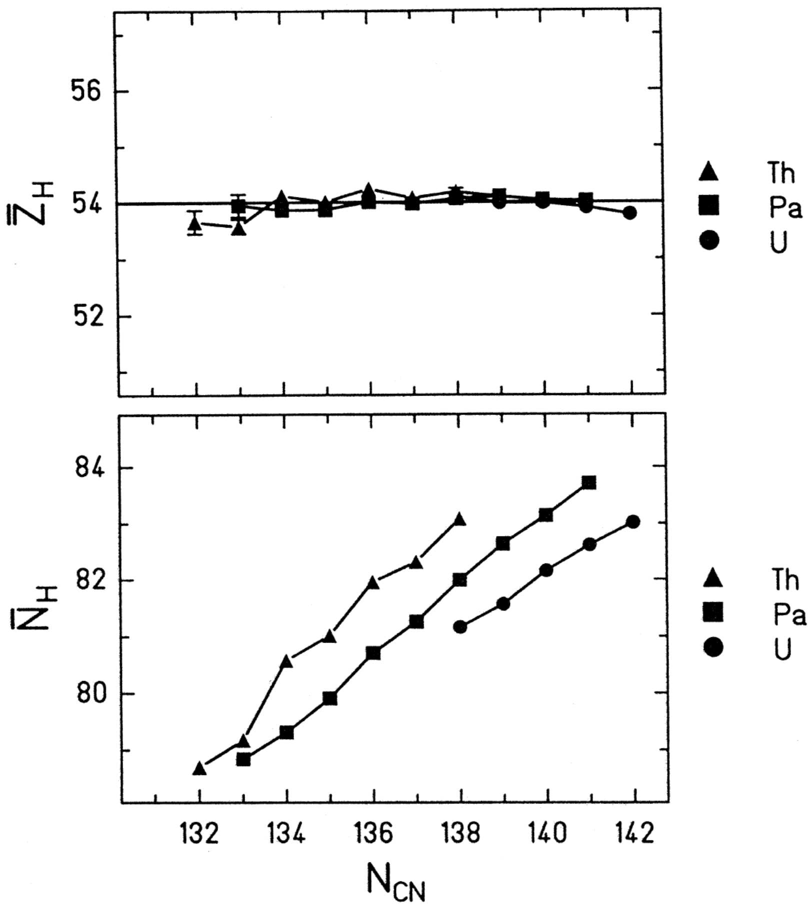


Mean position of the heavy asymmetric component in charge number (upper part) and neutron number (lower part)

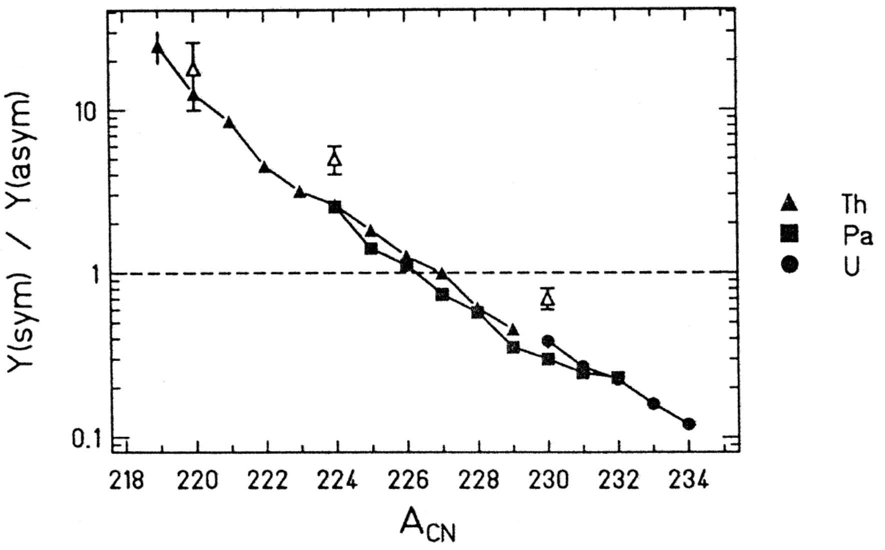


Intensity ratios of the symmetric and the asymmetric fission components in the transitional region as a function of mass number

# Low-energy fission: GSI (SOFIA)

L. Audouin et al., Nuclear Physics and Gamma-Ray Sources…, World Scientific Publishing, Singapore 2014 pp. 217-225

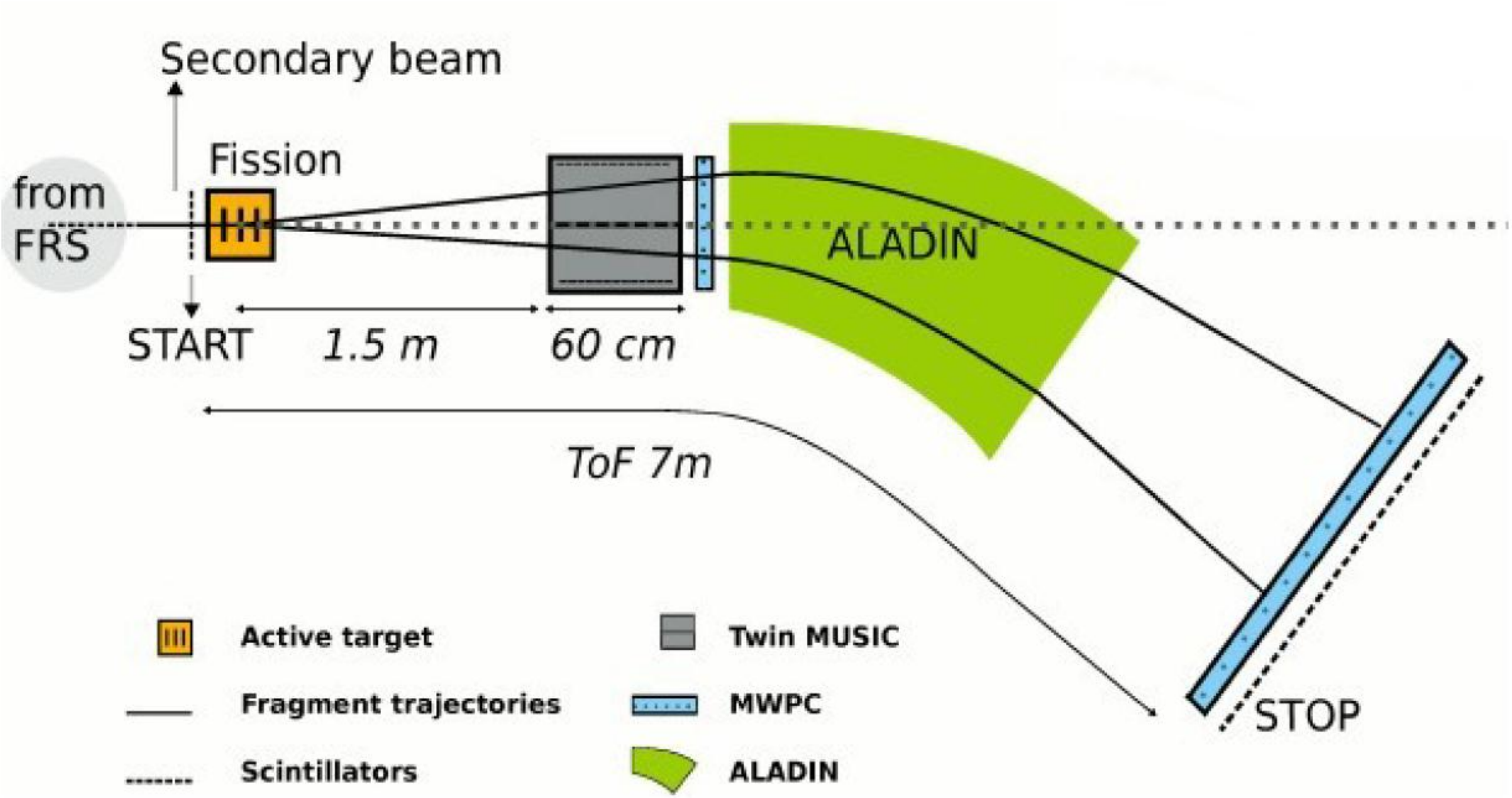


Scheme of the SOFIA (Study On Fission with Aladin) detection set-up for fission fragments.

# Low-energy fission: GSI (SOFIA)

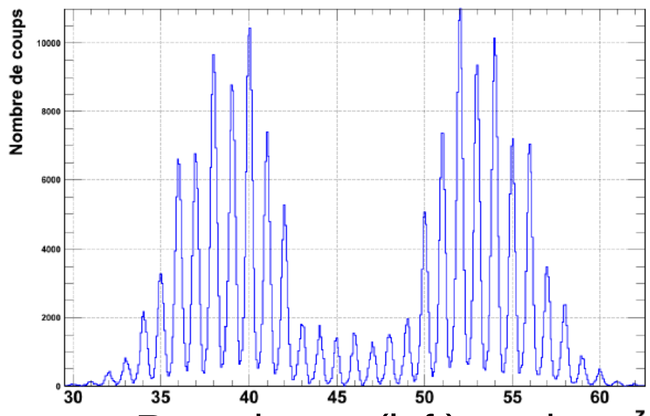


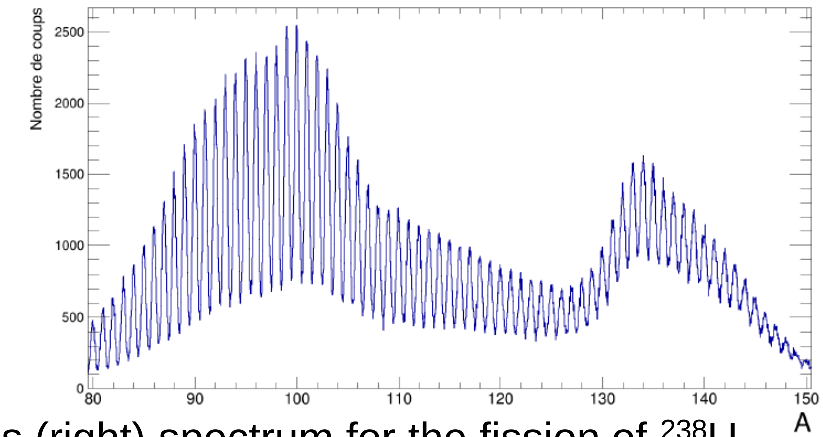


Raw charge (left) and mass (right) spectrum for the fission of $^{238}$U.

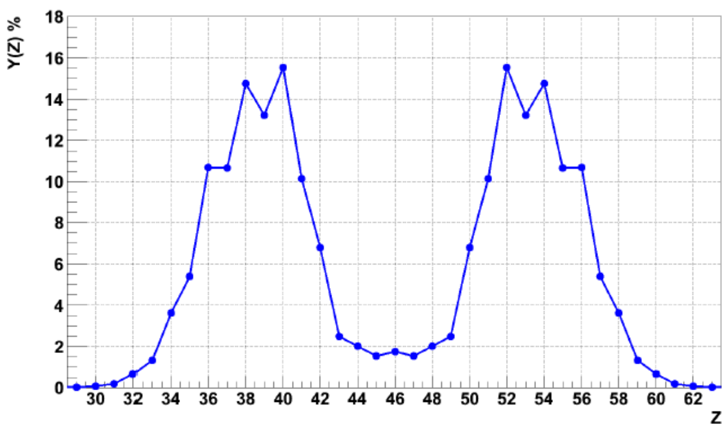


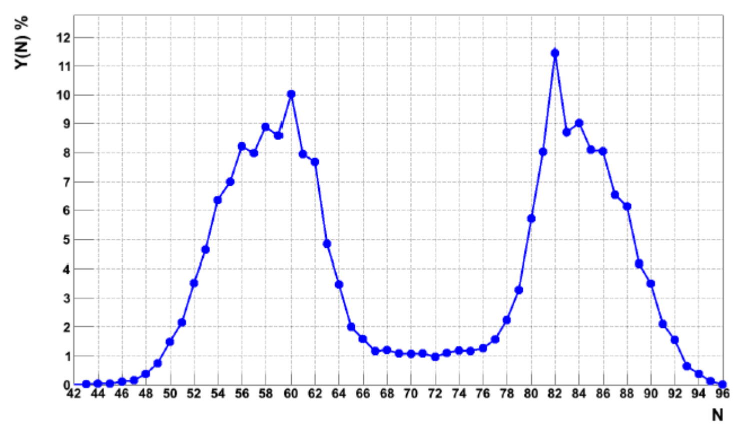


Elemental (left) and isotonic (right) yields for the fission of $^{238}$U.

# Low-energy fission: GSI (SOFIA)

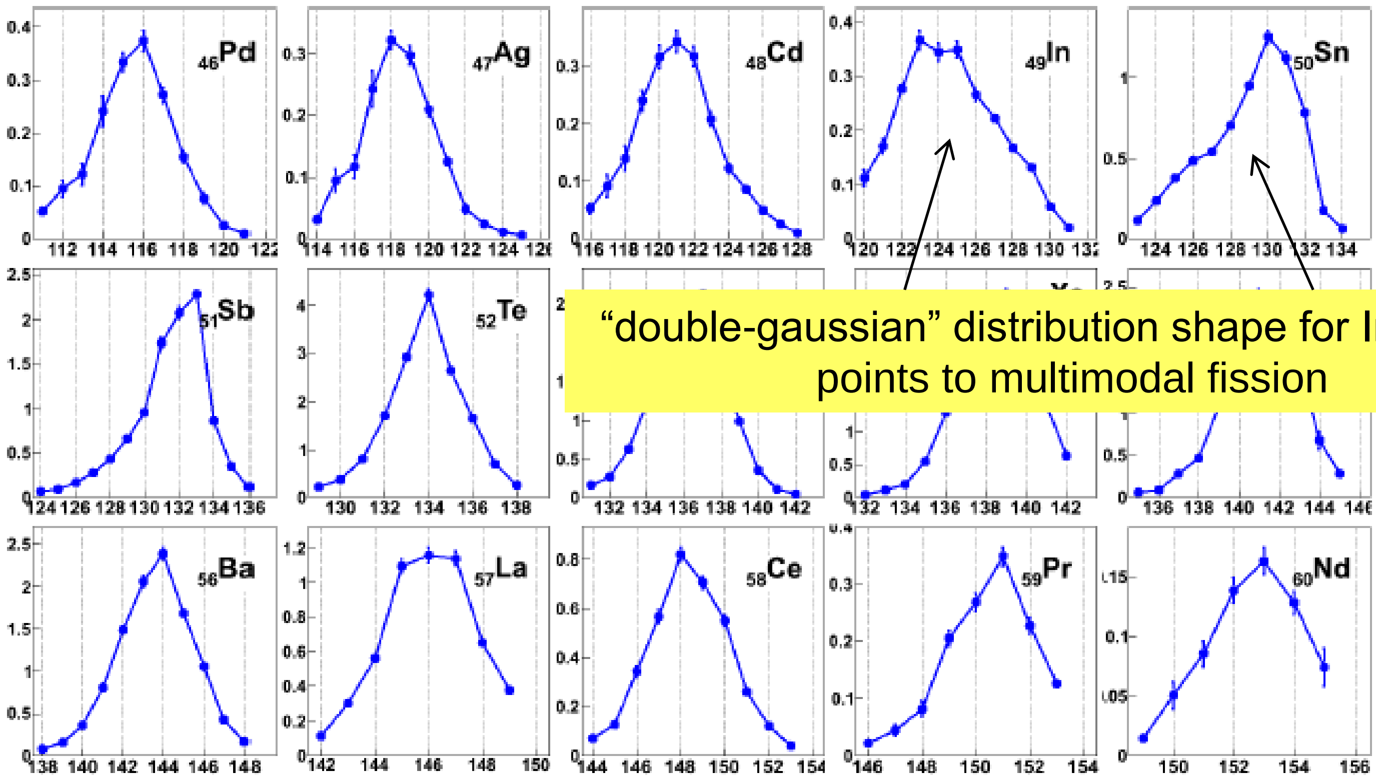


Isotopic yields for the electromagnetic-induced fission of $^{238}U$

The transition of shape in the In-Sn-Sb distributions corresponds to the transition between the fission modes: "super-long" (SL; deformed fragments) for Z<50 and "standard" (SI; spherical heavy fragment) for Z>50

# Low-energy fission: GSI (SOFIA)

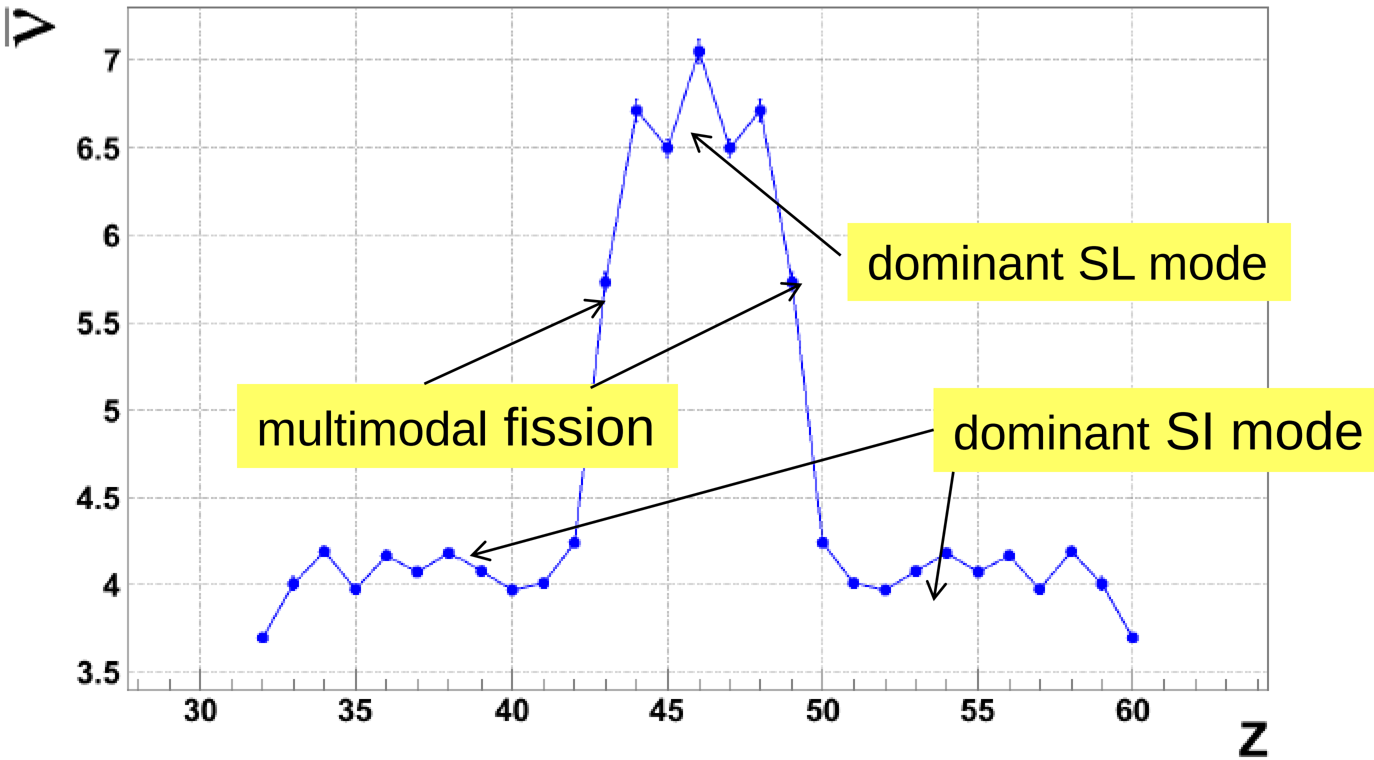


Average neutron emission as a function of Z

After an SL-mode fission, the deformation energy is converted in excitation and finally in additional neutron emission.